PALEOCEANOGRAPHIC MAPPING PROJECT
PROGRESS REPORT No. 43 - 0888

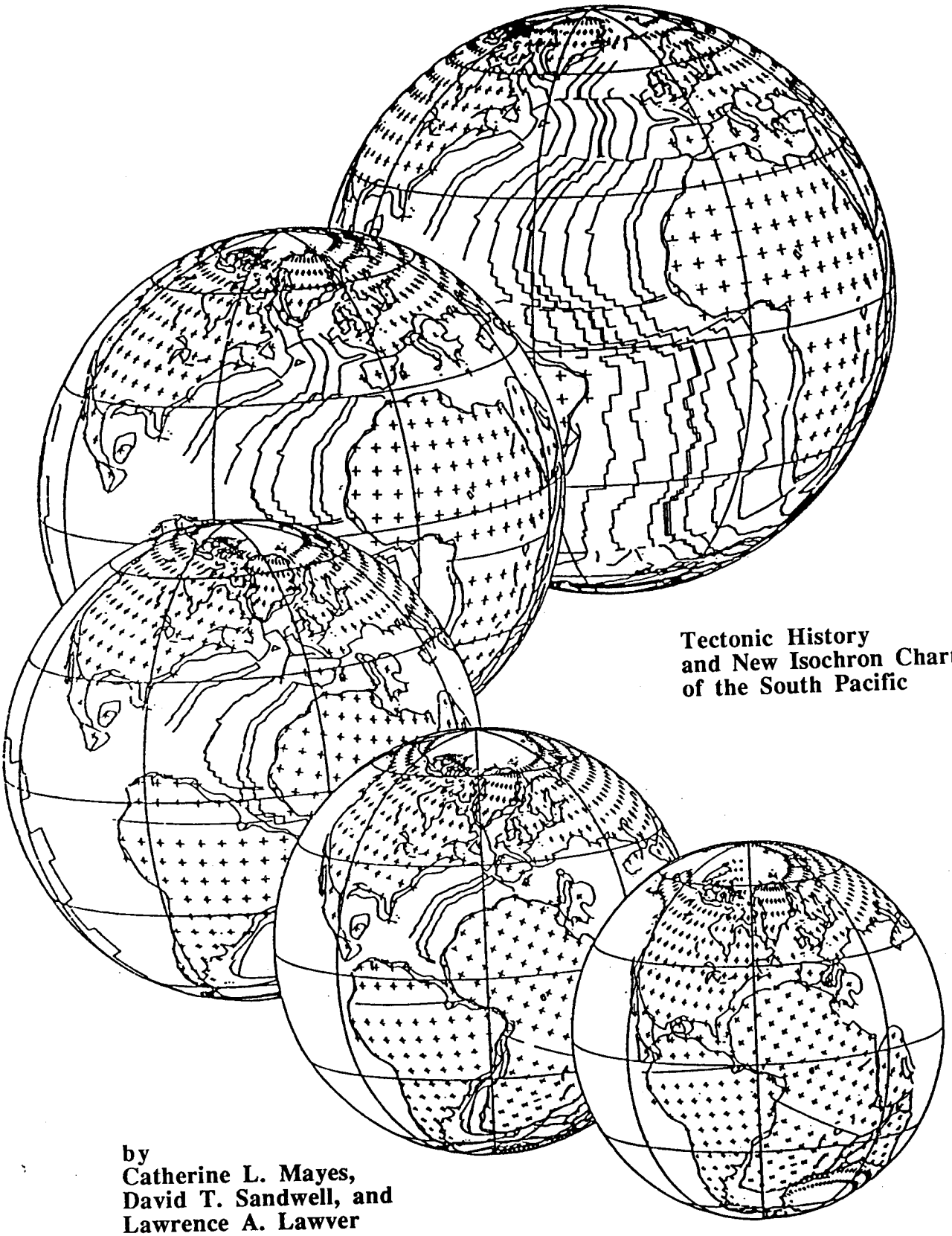

Tectonic History and New Isochron Chart of the South Pacific

by
Catherine L. Mayes,
David T. Sandwell, and
Lawrence A. Lawver

University of Texas Institute for Geophysics Technical Report No. 95

TECTONIC HISTORY AND NEW ISOCHRON CHART OF THE SOUTH PACIFIC

Catherine L. Mayes [1,2]

David T. Sandwell [2]

and

Lawrence A. Lawver [2]

[1] The Department of Geological Sciences and Instititue for Geophysics, P.O. Box 7456, University of Texas at Austin, Austin, Texas 78713-7456

[2] Institute for Geophysics, University of Texas at Austin, 8701 Mopac Blvd., Austin, Texas 78751

Submitted to:

Journal of Geophysical Research

May, 1988

ABSTRACT

We have developed an internally consistent isochron chart and a tectonic history of the South Pacific using a combination of new satellite altimeter data and shipboard magnetic and bathymetric data. Highly accurate, vertical deflection profiles (1-2 μrad), derived from 22 repeat cycles of Geosat altimetry, reveal subtle lineations in the gravity field associated with the South Pacific fracture zones. These fracture zone lineations are correlated with sparse shipboard bathymetric identifications of fracture zones and thus can be used to determine paleo-spreading directions in uncharted areas. The high density of Geosat altimeter profiles reveals previously unknown details in paleo-spreading directions on all of the major plates. Magnetic anomaly identifications and magnetic lineation interpretations from published sources were combined with these fracture zone lineations to produce a tectonic fabric map. The tectonic fabric was then used to derive new plate reconstructions for twelve selected times in the Late Cretaceous and Cenozoic. This is the first time that the tectonic history of the entire South Pacific has been studied as a whole. From our reconstructions, we estimated the former location of the spreading centers in order to derive a new set of isochrons (interpreted lines of equal age on the ocean floor). We believe that the use of new Geosat altimeter data in combination with a multi-plate reconstruction has led to a major improvement in our understanding of South Pacific tectonics.

There are three times of important changes in the tectonic history of the South Pacific. Just prior to Chron 34 (84.0 Ma) spreading initiated between Marie Byrd Land and the New Zealand block (the Campbell Plateau and the Chatham Rise). Spreading in the southwest Pacific was occurring along two different spreading centers between Chron 34 (84.0 Ma) and Chron 25 (58.9 Ma): the Pacific-Antarctic Spreading Center to the west and the Pacific-Bellingshausen Spreading Center to the east. At around the time of Chron 21 (49.4 Ma), the eastern and western spreading centers began spreading about a common pole of rotation. In addition, the Pacific-Antarctic Spreading Center broke through old crust to the north, transferring a piece of crust created at the

Pacific-Aluk spreading center to the Antarctic plate. The next major change in the South Pacific occurred between Chron 7 (25.8 Ma) and Chron 5 (10.6 Ma) when spreading initiated at the Galapagos Spreading Center and the East Pacific Rise was reoriented from spreading in a northwesterly direction to spreading in a northeasterly direction.

INTRODUCTION

The South Pacific covers 75 x 10^6 km^2 and represents one-sixth of the world's oceans. Our study area (75 degrees of latitude by 110 degrees of longitude) includes four major plates (Pacific, Antarctic, Cocos and Nazca). It is bordered to the east by Central and South America, to the south by Antarctica, to the west by the Macquarie Ridge, New Zealand and the Tonga-Kermadec Trench system, and to the north by the equator (Fig. 1). Whereas past studies have focused on one or two of the spreading centers in the South Pacific, we have attempted to summarize the tectonic history of the entire region from the Early Cretaceous to the present in an internally consistent model, and to identify any problems that might result from the combination of individual models incorporated into this project.

Because the area is so vast and remote, ship track coverage of bathymetry and magnetics is highly variable and frequently sparse . In some parts of the South Pacific for example along the northern East Pacific Rise, there are over 50 ship tracks per million square km, but these tracks are not uniformly-spaced across the area. In the south-central part of the region, however, there are only 6 to 26 nonuniformly-spaced tracks per million square km. We have been able to greatly-improve the coverage of the South Pacific by using satellite altimeter measurements of the marine gravity field collected by Geosat. To further improve the accuracy, resolution and coverage of the Geosat profiles, we have averaged 22 repeat cycles from the first year of the exact repeat mission. In this data set, there are 36 uniformly-spaced tracks per million square km near the equator increasing to more than 70 tracks per million square km at high latitudes. The average track spacing of the Geosat data is 82 km at the equator, and decreases to less than 40 km at high latitudes (McConathy and Kilgus, 1987).

Geosat measures the topography of the sea surface, which is nearly an equipotential surface of the earth's gravity field called the geoid. Variations in sea surface topography reflect mass deficits and surpluses associated with seafloor topography. Features such as seamounts, troughs and

fracture zones produce characteristic signatures in the sea surface topography with amplitudes well above the noise level of the satellite altimeter (Fig. 2). For example, an oceanic fracture zone produces a step in the sea surface that can be traced across many Geosat altimeter profiles. These fracture zone lineations correspond to tectonic flowlines and thus record the direction of the relative plate motion. Subtle changes in the trends of the flowlines reflect changes in the stage poles of relative motion between the plates. A combination of paleo-spreading directions (from Geosat data) and spreading rate information (from magnetic anomaly identifications) allows us to derive a more internally consistent model of the plate motion.

To derive the tectonic model, we first compiled and summarized previous studies of the South Pacific. We then identified fracture zone lineations on vertical deflection profile maps derived from Geosat altimeter data. We combined published magnetic anomaly identifications with the fracture zone lineations to construct a new tectonic chart. The digitized data were separated into tectonic elements (plates) and displayed on an interactive graphics terminal where each plate can be rotated around its pole. Using this interactive terminal, a set of self-consistent stage poles were determined for all of the plate pairs at each of 12 times. The tectonic reconstruction of the South Pacific at a particular time is the sum of the stage poles from the present to that time. From the past positions of the spreading centers at each time, we derived an isochron chart of the entire South Pacific.

Our study has implications for several fields: global plate motion circuits, the evolution of the Antarctic and Andean margins, plate motions in New Zealand, and ocean circulation. This work can be used to predict the age of unexplored or uninterpreted parts of the South Pacific. A regional tectonic study of the South Pacific can be used to constrain certain geologic problems along its margins. For instance, consideration of Antarctic-Pacific motion, combined with data concerning Antarctic-Australia motion, can help define the motion between the northern and southern parts of New Zealand and the history of the opening of the Ross Sea between East and West Antarctica.

Such consideration also has implications for the history of the Antarctic margin.

TECTONIC SETTING

The South Pacific is composed of four major plates: the Pacific, the Antarctic, the Nazca and the Cocos. The Pacific plate is the largest of all the plates. It comprises virtually all of the ocean floor in the Pacific north of the equator and two-thirds of the Pacific ocean floor south of the equator. It has been in existence since at least the Jurassic (Larson, 1976). In the area south of the equator, the oldest identified magnetic anomaly is Early Cretaceous (M17, 144 Ma, Larson, 1976). The Pacific plate is separated from the Cocos and Nazca plates by the East Pacific Rise (Menard, 1960, 1966; Sclater et al., 1971; Herron, 1972; Anderson and Sclater, 1972; Handschumacher, 1976; Klitgord and Mammerickx, 1982; Pardo-Casas and Molnar, 1987; Rosa and Molnar, 1988), and from the Antarctic plate by the Pacific-Antarctic Rise (Pitman et al., 1968; Molnar et al., 1975; Weissel and Hayes, 1977; Christoffel and Falconer, 1972; Cande et al., 1982; Stock and Molnar, 1987). For the Late Cretaceous to the present, identifiable marine magnetic anomalies and fracture zone trends define the spreading history of the Pacific fairly well. The older crust, created during the Cretaceous Quiet Zone (118 to 90 Ma), has very smooth bathymetry and little magnetic signature. This older crust is located just to the east of the Tonga trench (Fig. 2). The tectonic history of this region can only be surmised.

Some of the major features on the Pacific plate, other than the spreading ridges that define the major plate boundaries, are the seamount chains and plateaus (Fig. 1). In the northern South Pacific, the Marquesas, Tuamotu and Austral Islands appear to be located on a bathymetric high on the GEBCO 5.11 bathymetry chart (Mammerickx and Smith, 1984b). Further to the west, the Manihiki Plateau rises 2500 m above the surrounding sea floor. It is composed of oceanic material (Lanphere and Dalrymple, 1976). In the southwest Pacific, the Louisville Ridge is a nearly unbroken chain of seamounts extending from the Tonga-Kermadec Trench to about 46°S, 157°W.

The Antarctic plate is the second-largest constituent of the South Pacific seafloor. The tectonic history of crust currently attached to the Antarctic plate is complex. There is evidence for major ridge jumps and substantial ridge reorientations. Significant parts of the oceanic crust of the Antarctic plate are covered with ice year-round, so the historical record of the Antarctic plate is incomplete. The oldest remaining part of the Antarctic plate in the South Pacific is probably Late Cretaceous in age (Barker, 1982; Cande et al., 1982). The Antarctic plate is separated from the Nazca plate by an active spreading center, the Chile Rise (Cande et al., 1982; Cande and Leslie, 1986).

The current Antarctic plate can be split into two major pieces, East Antarctica and West Antarctica. West Antarctica is composed of several blocks (Grunow et al., 1987): the West Antarctic Peninsula block, the Ellsworth-Whitmore Mountains block, the Haag Nunataks block, the Thurston Island-Eights Coast block and Marie Byrd Land. Using the paleomagnetic results of Grunow et al. (1987), we are treating the West Antarctic blocks as one entity, Weddellia, from the Middle Cretaceous to the present. We use the Transantarctic Mountain Front as the division between East and West Antarctica (Dalziel, pers. comm.).

The Cocos and Nazca plates are the remnants of the older Farallon plate. These two plates are spreading apart along the east-west-trending Galapagos Spreading Center (Hey, 1977; Klitgord and Lonsdale, 1978; Klitgord and Mammerickx, 1982). Magnetic anomalies created at the old Pacific-Farallon spreading center are preserved on the Nazca plate close to the South American margin (Fig. 2). Between the East Pacific Rise (EPR) and the South American margin (5° to 17°S and 95° to 97°W), the Galapagos Rise forms a linear topographic high which was interpreted as a failed spreading center by Anderson and Sclater (1972) and Mammerickx et al. (1980). Because the EPR is spreading in an east-west direction near the equator and extruded basalt is only weakly magnetized in a direction perpendicular to the seafloor, it is difficult identify magnetic anomalies. Therefore, the age and spreading history of crust on parts of the Nazca plate remain ill-defined.

The ages of much of the Cocos plate also remain unknown.

The spreading centers separating the plates are offset by numerous fracture zones. The Pacific-Antarctic Rise boundary contains very-large-offset fracture zones which are apparent on bathymetric charts (Fig. 1), even with the very limited coverage in this region. The Eltanin Fracture Zone system (Fig. 2) is the most remarkable of these features. This system consists of two major fracture zones, the Heezen and the Tharp Fracture Zones, along with several fracture zones with smaller offsets. The Heezen Fracture Zone offsets the ridge by 350 km; the Tharp Fracture Zone has a larger offset of 650 km. Immediately to the north and south of the Eltanin system, the Menard and Udinstev Fracture Zones also have large offsets on the Pacific-Antarctic Rise. The Chile Rise is offset by two major fracture zones: the Valdivia Fracture Zone at 41° S and the Guafo Fracture Zone at 45° S (Fig. 2). The northern plate boundary between the Nazca and Antarctic plates is also a large-offset fracture zone called the Chile Fracture Zone. The length of the Chile Fracture Zone is approximately 800 km. The fracture zones along the EPR and the Galapagos Spreading Center are relatively small-offset fracture zones, with most offsets less than 150 km, as opposed to the 300 km offset of the Udinstev Fracture Zone along the Pacific-Antarctic Ridge.

Two microplates have been identified in the South Pacific. Between 22° and 27° S on the EPR (Fig. 2), a new ridge has developed to the east of the old EPR (Handschumacher et al., 1981). The EPR appears to be in the process of jumping from the old ridge, Oeste (Spanish for West), 400 km to the east to the new ridge named Este (Sp.: East). This ridge jump defines the Easter microplate which appears to have been in existence for 3.2 million years. The Juan Fernandez microplate between 31° and 35° S is defined by bathymetry and earthquakes at the Pacific-Nazca-Antarctic triple junction (Anderson-Fontana et al., 1986). The EPR is again jumping from the West Ridge to the East Ridge, with spreading having initiated on the East Ridge about 3 Ma (Fig. 2). There are at least two older major ridge jumps in the South Pacific region which will be

discussed later.

The South Pacific region is bordered by a combination of trenches, transform faults, and passive margins. The plate boundary between the Pacific and Indo-Australian plates is convergent or transpressional along different parts of the plate boundary (Kamp, 1986). This plate boundary trends north along the Macquarie Ridge and through New Zealand along the Alpine Fault (Fig. 1).

Bordering the Pacific crust to the west is the Tonga-Kermadec Trench system. There have probably been subduction zones to the west of the Pacific spreading regimes since at least the Cretaceous. The Lord Howe Rise (Fig. 1a), a submerged block of continental crustal thickness, is probably related to subduction. Its composition is rhyolite (Burns et al., 1973). The Lord Howe Rise can be reconstructed to Australia by closing the Tasman Sea (Hayes and Ringis, 1973; Weissel and Hayes, 1977). Back-arc spreading which formed the marginal basins of the South Pacific is probably responsible for reorienting the trench into its current position (Karig, 1970). The Vitiaz-Solomon-New Britain Trench system forms the remaining boundary of the Pacific plate.

Along the eastern margin of the Pacific Ocean basin, Cocos, Nazca and Antarctic crust is being subducted beneath Central and South America along the Middle America and Peru-Chile trenches. We estimate that the Peru-Chile Trench has consumed at least 6000 km of Farallon, Nazca and Cocos plates. The Shackleton Transform Fault, which trends from the southern tip of South America to the northern tip of the West Antarctic Peninsula, forms the boundary between the Antarctic-Drake spreading regimes and the spreading system of the Scotia Sea. The Pacific margin of West Antarctica can be split into three segments. From the Shackleton Fracture Zone to the Hero Fracture Zone, the margin is characterized as a recently convergent margin which resulted in subduction of the Drake plate beneath the West Antarctic Peninsula (Barker, 1982). Backarc basin extension is still active in the Bransfield Straits, although the arc is no longer active (Barker, 1982). The segment of the margin between the Hero Fracture Zone and Pine Island Bay was once

a subducting margin (Barker, 1982). There have been a series of ridge-trench collisions at different times along the margin which resulted in motion ceasing between West Antarctica and the oceanic crust immediately to the north (Herron and Tucholke, 1976; Barker, 1982). The western-most segment of the West Antarctic margin is adjacent to Marie Byrd Land and lies between Pine Island Bay and the Ross Sea. This segment is the conjugate passive margin to the Campbell Plateau and the Chatham Rise (offshore New Zealand) to the north (Molnar et al., 1975; Crook and Belbin, 1978; Stock and Molnar, 1987; Grindley and Davey, 1982).

DATA

A. COMPILATION OF SHIPBOARD MAGNETIC AND BATHYMETRIC DATA

The shipboard data used in our reconstructions consist of previously identified magnetic anomalies, interpreted magnetic lineations and identified fracture zone crossings (Fig. 2). We have not re-identified any magnetic anomalies. Therefore, there may be inconsistencies in our model because different authors picked different parts of the magnetic anomalies (i.e. peaks, troughs or inflection points). In our compilation of shipboard data, we have used the lineation pattern and fracture zone identifications of Klitgord and Mammerickx (1982) for the northern East Pacific Rise and the Galapagos Spreading Center. For the Galapagos Rise, we used the interpretations of Mammerickx et al. (1980). For the southern East Pacific Rise, we used the lineations of Handschumacher (1976) and some identifications from Herron (1972). For the older mid-Tertiary anomalies along the old Pacific-Farallon spreading center, we used the identifications and fracture zones from Pardo-Casas and Molnar (1987), while the oldest anomalies on the Pacific-Farallon spreading center were taken from Cande et al. (1982). On the Chile Rise, we have used the identifications of Cande et al. (1982) and Cande and Leslie (1986). In the south, we have used anomaly identifications and lineations from Molnar et al. (1975), Weissel et al. (1977), Cande et al. (1982) , Christoffel and Falconer (1972) and Stock and Molnar (1987) for anomalies along the

Pacific-Antarctic Rise. Along the Antarctic margin, we used the identifications of Herron and Tucholke (1976) and Barker (1982).

Because the South Pacific is such an immense region and because many parts of the area are far from ship ports, ship track coverage in the South Pacific region is highly variable. There are many large areas between fracture zones with no magnetic picks or lineations. Also, many published fracture zone lineations have not been sampled finely enough to represent the true trends and complexities of fracture zones in the South Pacific. Consequently, we have used satellite altimetry data to give us more detail in order to define relative plate motion.

B. VERTICAL DEFLECTION FABRIC CHART (GEOSAT)

Sandwell and Schubert (1982), Sailor and Okal (1983), Haxby (1987), Cande et al. (in press), Craig and Sandwell (in press), and Okal and Cazenave (1985) used satellite altimetry data to locate seafloor features and trace tectonic lineations. All of these papers use data from the Seasat instrument. Data from the Geosat (GEOdesy SATellite) have a higher degree of accuracy than equivalent Seasat data. Geosat data achieved an accuracy of 3.5 cm for significant wave heights of 2 m (McConathy and Kilgus, 1987; MacArthur et al., 1987), better by a factor of 2.9 than the 10 cm accuracy of Seasat data for wave heights less than 20 m (Tapley et al., 1982). The Geosat began its unclassified Exact Repeat Mission (ERM) in October, 1987, and was in operation during the Austral summer, 1987/88, unlike the Seasat satellite which lasted only 3 months before the satellite failed in October, 1978. During the Austral summer, the sea ice around Antarctica is at a minimum and Geosat recorded a geoid signal in high southern latitudes, which is noteworthy because of the sparse ship track coverage in the area (Sandwell and McAdoo, in press). Since Geosat has been placed in the unclassified 17-day ERM, it has an equatorial track spacing of 164 km (McConathy and Kilgus, 1987). We have averaged 22 of these Geosat altimeter repeat cycles to further improve the data accuracy and coverage in the South Pacific region.

The Geosat data consist of two directions of satellite passes: ascending (those travelling from southeast to northwest) and descending (those traveling from northeast to southwest) (Fig. 3). We use a combination of ascending and descending passes to make our interpretations. The main interest of our study is the identification of tectonic flowlines. Since the flowlines are generated by features which have relatively short wavelengths in the geoid, the slope of the geoid is used rather than the geoid itself. The first derivative of the geoid, or the slope, is called the deflection of the vertical. The vertical deflection is plotted perpendicular to the ground tracks (Fig. 3). The data were filtered by a Gaussian filter to remove wavelengths shorter than 19.8 km. The longest wavelengths (greater than 4000 km) were also removed using the spherical harmonic coefficients of the PGS-54 gravity model (Marsh and Martin, 1982). Filtering of the data was done for two reasons: the shorter wavelengths are filtered out because they are below the threshold of noise; the longer wavelengths are related to deep-seated gravity anomalies and thermal convection and therefore presumed not to be a reflection of the bathymetry.

Seamounts and trenches are picked at the zero crossing between peaks and troughs on plots of the deflection of the vertical (Fig. 4a). Since the gravity signatures of fracture zones vary with spreading rate (Shaw and Cande, 1987), we use the satellite altimetry data to predict spreading direction by determining tectonic flowlines, rather than by locating the fracture zones themselves. Flowlines indicate the direction of relative plate motion, and we can use these just as we use fracture zone identifications to constrain reconstructions.

Plots of the deflection of the vertical along satellite track were used to make our fabric map. The peaks and troughs of the vertical deflection are traced from track to track, in much the same way as seismic lines are interpreted. Lineations were traced on the basis of polarity, amplitude and character. These lineations comprise the vertical deflection fabric chart (Fig. 5). For a feature in the Geosat data to be considered a lineation, it must cross at least three tracks. On the vertical deflection fabric chart, our interpreted lineations correlate well with the bathymetric fracture zone

identifications of the Eltanin fracture zone system from the GEBCO charts (Fig. 6, after Mammerickx et al., 1984). The vertical deflection fabric chart actually gives more detail for the trends of the fracture zones because the Geosat tracks are more numerous and more uniformly-spaced than the available ship tracks. The Geosat data are, however, limited because the amplitude of the geoid signal over a feature is dependent on the angle between the satellite track and the trend of the feature. Because of this, some bathymetric features, for example fracture zones which trend parallel to a satellite track, will not be recorded by the Geosat instrument.

Several striking features are apparent on the vertical deflection fabric chart (Fig. 5). As discussed earlier, the Eltanin Fracture Zone System (Figs. 5 and 6) consists of two large fracture zones, the Heezen and the Tharp, and several smaller fracture zones (Molnar et al., 1975). The distance between the Heezen and Tharp fracture zones changes along their length (Fig. 6). Indeed, on the gridded and averaged Seasat map by Haxby (1987), it appears as if these two fracture zones become one feature to the north and south of the active ridge. From the Geosat data, however, it can be seen that the Heezen and Tharp Fracture Zones remain two distinct features (see Fig. 6b).

The Heezen and Tharp Fracture Zones diverge to the north and south beginning at about 700 km from the present-day ridge. As the lineations from the two fracture zones diverge, a secondary feature appears between them, both to the north and to the south. In the north, the feature between the fracture zones has a negative slope. In the south, the secondary feature is a region of positive slope. These features may be edge effects in the geoid caused by the small distance between the fracture zone lineations, about 43 km. However, the positive lineation in the southern zone and the negative lineation in the northern zone have trends which, when reconstructed, appear to be parallel to each other and to the small circles about the stage pole for Anomaly 7 to Anomaly 10. These features may reflect an intermediate stage in the development of the relative motion between the Antarctic and Pacific plates.

Between the equator and 30°S, the observed vertical deflection lineations have two distinct

orientations (Fig. 3a and b). More recent seamount chains cut across an older fabric which can be related to seafloor spreading. The seamount chains trend to the northwest while the older fabric trends to the northeast. In addition, the number of identifiable lineations which are parallel to the older fabric is comparatively small because the ocean floor in this region was created at a very fast spreading center (160 mm/yr along the Pacific-Nazca (Farallon) spreading center) (Handschumacher, 1976).

The Sala y Gomez Ridge lies in the eastern South Pacific at 25° S on the Nazca plate. This feature consists of a line of seamounts and ridges on top of anomalously shallow crust. Bonatti et al. (1977) interpreted this feature as a hotspot trace. Mammerickx (1981) and Mammerickx and Sandwell (1986) have suggested on the basis of its complex nature in the Seasat data that the Sala y Gomez Ridge is an incipient rift, analogous to the Galapagos Spreading Center further to the north. We observe the same complexity in the Geosat data.

The Henry Trough on the Pacific plate (46° S, 135° W) and the Hudson Trough on the Antarctic plate (55° S, 95° W) are bathymetric troughs which were identified in the Seasat data by Mammerickx and Sandwell (1986). They can also be seen in the Geosat data and lineation charts (Figs. 3b and 5). The Henry Trough, which is crossed by 8 Geosat tracks, has a NE-SW orientation. Five Geosat tracks cross the Hudson Trough; it trends roughly north-south. These two features are interpreted as scars left when a younger spreading center broke through older crust (Cande et al., 1982).

Differences in spreading rate are observed along the spreading centers during various periods in the past. Close to the Pacific-Antarctic Ridge, the Geosat signal is relatively flat, indicating smooth topography and a fast spreading rate (Fig. 3). At about the location of Anomaly 7 identifications on the Pacific-Antarctic Ridge, the Geosat data show a larger number of peaks and troughs. These can be traced from track to track as geoid fabric lineations. This indicates that the the topography is rougher and the spreading rate was slower. Close to the Campbell Plateau

margin, the Geosat signal becomes quiet, indicating another change in the past spreading rate. The sparseness of tectonic flowlines identifiable on the Pacific-Nazca (Farallon) Spreading Center reflects the very fast spreading rate along that ridge.

TECTONIC CHART

Regionally continuous vertical deflection lineations, individual magnetic anomaly identifications and magnetic lineations, and bathymetric features taken from the GEBCO map series (Mammerickx and Smith, 1984a and b; Mammerickx et al., 1984; Falconer and Tharp, 1984; Johnson and Vanney, 1984; Monahan et al., 1984) were combined to produce a tectonic fabric chart (Fig. 7). We used the vertical deflection lineations that could be traced from track to track over long distances for the purpose of calculating new poles of rotation. The fracture zones lineations that were used are associated with the Heezen and Tharp fracture zones in the Eltanin system, the Udinstev, the Menard and the Chile fracture zones. The signals from the fracture zones along the length of the Chile Rise are useful because they also are continuous and have a strong signal. Along the southern EPR (from the Pacific-Nazca-Cocos triple junction to the Pacific-Nazca-Antarctic triple junction) and the Galapagos Spreading Center, the fracture zones have much smaller offsets, and do not have the age contrasts on either side of the fracture zones as large as the contrasts on the larger-offset fracture zones. For this reason, these fracture zones do not have a strong Geosat signal. An additional problem along the Galapagos Spreading Center is the north-south orientation of the fracture zones and their short lengths. Each fracture zone would appear on only one track, making it impossible to use the Geosat data to give the trends of these fracture zones. We have therefore used the fracture zone identifications from the GEBCO charts 5.7 and 5.11 (Mammerickx and Smith, 1984a and b), Handschumacher (1976) and Klitgord and Mammerickx (1982) for our tectonic chart.

On the tectonic fabric chart (Fig. 7), a flowline lineation representing a large-offset fracture

zone, such as the Heezen or the Tharp, is composed of a lineation of maximum positive slope on one side of the active ridge and a lineation of maximum negative slope of the other side. These lineations represent a step up in topography on one side of the active transform from older crust to younger crust and a step down from younger to older on the other (Fig. 4b). We feel that using the vertical deflection lineations, in conjunction with the bathymetric identifications, to constrain the spreading direction is a better method for calculating poles of rotation than using the bathymetric identifications alone because the vertical deflection lineations have in many cases a much denser and generally more uniform sampling than lineations determined on the basis of bathymetric identifications.

RECONSTRUCTION METHODS

After compiling the data, we used an Evans and Sutherland PS300 interactive graphics system to reconstruct the plate locations through time (Scotese et al., in press). We separated the digitized data by assigning them to individual tectonic elements, or plates. Each tectonic element can be displayed and independently rotated around any pole of rotation relative to any of the other plates displayed on the surface of a virtual sphere. Plate rotations are determined based on the best visual fit of the data. We used a computer program which utilized the hierarchical tectonic analysis technique on an interactive graphics terminal (Ross and Scotese, in press) to reconstruct the plates to their relative positions in the past. The reconstructions were done beginning with the present and working backward in time, using the younger reconstructions as starting points for older reconstructions.

Our method for calculating the poles of rotation which move plates into their relative positions in the past uses a combination of the concepts of finite poles and stage poles. The finite pole of rotation for a plate pair is the Euler pole which reconstructs one plate relative to the other from its present-day relative position to its relative position for some time in the past. The sum of a series

of stage poles which represent the relative motion between two plates for discrete periods of a longer interval equals the finite pole for that interval. For example, in calculating a pole for Chron 10 for Pacific-Antarctic motion, we first reconstructed the Antarctic plate to the Chron 7 position, relative to a Pacific plate fixed in present-day coordinates. We then moved the Pacific plate relative to the reconstructed Antarctic plate, matching Anomaly 10 identifications, lineations and flowlines on each plate. To reconstruct the Chron 10 position of the Pacific plate with respect to the Antarctic plate, the Pacific plate must be moved to the Antarctic plate by the Chron 10 to Chron 7 stage pole for Pacific-Antarctic motion. By using the stage poles, we utilized the tectonic fabric lineations as flowlines which record relative motion between the two plates during the specified time period. Accurate stage poles are derived by matching not only the corresponding magnetic anomaly picks but also the lineations and their directions. This procedure assures us that the plates are being moved by a logical progression of stage poles. Finally, to calculate the finite pole for Chron 10, we added the stage pole for Chron 10 to Chron 7 to the finite pole for Chron 7.

In the cases where age identifications for only one side of a spreading ridge have been identified (i.e. when one plate has been subducted, is covered with ice, or has no magnetic anomaly identifications), a different procedure was used to calculate poles of rotation. In these cases, we rotated younger picks onto older anomalies using a stage pole which has small circles parallel to the direction of the tectonic flowlines. The angle used to move the younger anomaly on top of the older anomaly approximates the half angle for the stage pole of relative motion between the two plates. By doubling the angle and adding this stage pole to the finite pole for the younger anomaly, we calculated the finite pole of rotation for these anomalies. We used this method for Pacific-Farallon spreading older than Chron 13 and for Pacific-Antarctic spreading older than Chron 18.

To test the accuracy and self-consistency of the poles we determined, we calculated the spreading rates, directions and the stage poles for Pacific-Antarctic (Bellingshausen), Pacific-

Antarctic (Weddellia), and Pacific-Nazca (Farallon) plate pairs. Spreading rates and directions were plotted against time to give us a visual test of consistency and smoothness of changes in orientation and rate (Fig. 8). We plotted small circles for the entire length of the ridges in 1° intervals and compared the small circle trends with the trends of our tectonic fabric lineations. We then used the small circles and the matched anomaly picks and lineations, with additional constraints from ridges drawn for younger reconstructions, to draw the spreading center for a particular reconstruction. These spreading centers are assigned to their respective plates, and we use them as isochrons.

RECONSTRUCTIONS

We present reconstructions for twelve times in the past. The times of our reconstructions were selected because they have a relatively high number of magnetic anomaly identifications associated with them. We use the DNAG time scale (Berggren et al., 1985; Kent and Gradstein, 1985) to assign ages to our reconstructions (Table 1). The finite poles of rotation used are given in Table 2. The finite poles for Anomalies 5, 13, 25 and 31, for Pacific-Antarctic (Bellingshausen) fall within the uncertainty regions calculated in Stock and Molnar (1982) and Stock (pers. comm.). We make the distinction between an 'Anomaly' and the time of a particular anomaly by using the term 'Anomaly' the refer to the magnetic anomaly identification and 'Chron' to refer to the time of the anomaly, using the convention of Klitgord and Schouten (1986). For ease of presentation we begin with the oldest reconstruction and move forward in time.

A. EARLY AND LATE CRETACEOUS (144 - 90 Ma)

The early seafloor spreading history of the South Pacific remains a mystery. The oldest identified magnetic anomaly south of the equator is M17 (144 Ma) (Larson, 1976). Cretaceous crust is restricted to the northwest corner of the area just east of the southwest Pacific trench

systems (Fig. 2). This area has a history of seamount and plateau formation. The Line Islands, Solomon Islands, Tokelau Islands, and the Manihiki and Ontong-Java Plateaus are all in this area. Formation of plateaus and particularly the seamount chains obliterates the original magnetic fabric of the area. Consequently, dating the age of the seafloor using magnetic anomaly identifications is very difficult in this region (Mammerickx, pers. comm.). Much of the original tectonic fabric seen in the Geosat data has been overprinted and the only features which we have been able to identify from the geoid data are seamounts.

Larson (1976) identified Early Cretaceous magnetic lineations in the western equatorial Pacific. Winterer (1976) used these identifications and a bathymetric study to propose a history for the Early Cretaceous crust in the central Pacific. He suggested that the Nova Canton Trough, a subtle topographic feature trending ENE just south of the equator (Fig. 1), might be a failed spreading center. The east-west trending Phoenix lineations of Larson (1976) might have been created at this spreading center. Crust between the Nova Canton Trough and the Manihiki Plateau would then be the conjugate to the Phoenix lineations, and would increase in age to the south. According to Winterer (1976), spreading at the Nova Canton Trough ceased at approximately M0 time (120 Ma), and the ridge jumped south to form the Manihiki Plateau. The new spreading center became the Pacific-Aluk plate boundary and spread very rapidly. Lanphere and Dalrymple (1976) dated the Manihiki Plateau radiometrically at 110-120 Ma. The oldest sediments on the plateau contain fossils of Aptian age (119 Ma to 113 Ma) (McNulty, 1976). We estimate the spreading rate on the Pacific-Aluk to be 15.6 cm/yr along the Pacific-Aluk boundary using the magnetic anomaly identifications of Cande et al. (1982), and predict that approximately 2700 km of oceanic crust exists between identified Anomalies 34 and M0 on the Pacific plate. With this scenario, it is then possible to suggest that crust between Anomaly 34 of Cande et al. (1982) and the Manihiki Plateau was formed at the Pacific-Aluk spreading center during the Cretaceous Quiet Zone.

B. LATE CRETACEOUS TO PALEOCENE (90 - 58.9 Ma)

Seafloor spreading in the present-day southwest Pacific began at around Chron 34 (84.0 Ma). Prior to that time, seafloor spreading was occurring along the Pacific-Farallon boundary to the east and Pacific-Aluk plate boundary to the north (Fig. 9). The Aluk and Pacific plates were being subducted beneath New Zealand, the Chatham Rise and the Antarctic margin to the east of Pine Island Bay. New Zealand, the Chatham Rise and the Campbell Plateau were all part of Gondwanaland, with the Chatham Rise and Campbell Plateau having been contiguous to Marie Byrd Land (Grindley and Davey, 1982).

Christoffel and Falconer (1972) identified an 'Anomaly 36' just south of the Campbell Plateau and the Chatham Rise (Fig. 10). These 'Anomaly 36' identifications are actually Anomaly 34 according to the time scale of Berggren et al. (1985), after a discussion with Stock (personal communication) and a reanalysis of the location of the continental margin from the Geosat data. The 'Anomaly 36' identifications are located 75 km south of the ocean-continent boundary identified on the Geosat fabric map. On this basis, we propose that the Chatham Rise and the Campbell Plateau rifted away from Marie Byrd Land just prior to Chron 34 (84.0 Ma). The Bounty Trough is a depression between the Campbell Plateau and the Chatham Rise (Fig. 1a). Since both the Campbell Plateau and the Chatham Rise can be reconstructed to Marie Byrd Land with closure in the Bounty Trough, there must have been some relative motion between the Campbell Plateau and the Chatham Rise opening the Bounty Trough. The exact timing of the opening of the Bounty Trough is, however, unclear. At approximately the same time, subduction of the Aluk plate ceased between the Udinstev Fracture Zone and the Tharp Fracture Zone along the Thurston Island-Eights Coast segment of the Antarctic margin, perhaps as a result of the subduction of the western-most segment of the Pacific-Aluk spreading center. The spreading occurred in a direction of N10°W at a rate of about 40 mm/yr. We were unable to use our tectonic fabric map to determine spreading directions because the signal of the satellite altimetry data is very

smooth between the Campbell Plateau and the Anomaly 25 identifications to the south, perhaps because the offsets on the fracture zones in this area are small. A triple junction was active at 52° S and 173° W between the Pacific, Bellingshausen and Antarctic plates (Stock and Molnar, 1987). Evidence for this triple junction is preserved on the Pacific plate in a subtle magnetic bight south of the Bounty Trough (Molnar et al., 1975; Stock and Molnar, 1987). We applied a different finite pole to the northern section of what is now the Pacific-Antarctic Ridge using the identified magnetic anomalies and our tectonic fabric lineations and determined an average spreading azimuth of N20°W with a spreading rate of 50 mm/yr for Pacific-Bellingshausen spreading center. Our calculations show that the Antarctic-Bellingshausen plate boundary was a spreading center, making the triple junction a RRR type. Using a combination of tectonic fabric and picks and lineations by Molnar et al. (1975), Weissel et al.(1977), and Cande et al. (1982), we calculate a spreading azimuth of N60°W with an average rate of 50 mm/yr for Anomaly 21 (49.6 Ma) to Anomaly 31 (69.0 Ma) on the Pacific-Bellingshausen spreading center.

Prior to Chron 29 (65.8 Ma), a RRR triple junction developed between the Bellingshausen, Pacific and Aluk plates (Cande et al., 1982). As this triple junction migrated eastward, dual spreading centers were left behind. During the period between Chron 29 and Chron 25, the dual spreading centers jumped eastward in the southeast Pacific (Figs. 12 and 13). The two spreading centers, Pacific-Bellingshausen and Bellingshausen-Aluk, began spreading apart prior to Chron 29 between the Heezen and Tharp Fracture Zones. As they propagated eastward, the dual spreading centers then began spreading between the Tharp and Tula Fracture Zones just prior to Anomaly 28. Therefore, crust on the Bellingshausen Plate was being created further and further east. The active ridges accommodated the rapid motion between the Pacific and Aluk Plates on a dual spreading system. The spreading configuration with dual spreading occurring between both the Heezen and Tharp and the Tharp and Tula Fracture Zones and fast Pacific-Aluk spreading occurring to the north of the Tula Fracture Zone was a stable system from Chron 28 (64.3) to just prior to Chron

21 (49.6 Ma).

Between Pine Island Bay and the Tharp Fracture Zone (Figs. 1c and 2), the seafloor is now also directly coupled to the continental margin (Barker, 1982). In this location subduction stopped at about 90 Ma, as evidenced by the Late Cretaceous age for the youngest calc-alkaline igneous rocks in the Thurston Island block (Fig. 1c) of Antarctica (Storey et al., 1987). The Udinstev Fracture Zone fabric lineation can be traced from the Pacific-Antarctic Ridge southward to intersect Pine Island Bay, although identification becomes ambiguous close to the margin (Fig. 3a). This is evidence that the Udinstev Fracture Zone is a major boundary, and it suggests that there was subduction of the Aluk plate to the east but a passive margin of Marie Byrd Land to the west. The Udinstev Fracture Zone may represent the westernmost extent of the Aluk Plate. The youngest identified anomalies between the Tula Fracture Zone and the Udinstev Fracture Zone are Paleocene in age (Anomaly 22 to Anomaly 25) along the Bellingshausen-Aluk spreading center.

C. EOCENE: CHRON 21 (49.6 Ma)

At approximately 50 Ma, the spreading centers in the South Pacific underwent a major change in configuration (Fig. 14). Spreading along the Antarctic-Bellingshausen plate boundary ceased, and the Pacific-Antarctic spreading center south of the triple junction and Pacific-Bellingshausen spreading center to the north of it became one Pacific-Antarctic spreading center spreading with respect to a common pole (Stock and Molnar, 1987). Stock and Molnar (1987) date this change in configuration at Chron 18 (42.7 Ma). However, the change in geoid signal from smooth to the north to numerous lineations to the south occurs just south of the Anomaly 25 identifications of Christoffel and Falconer (1972) and Stock and Molnar (1987). Vertical deflection lineations which represent fracture zone trends south of Anomaly 25 are parallel to lineations further to the south on the Pacific plate. In addition, the picks and lineations of Molnar et al. (1975) allow us to use an orientation parallel to the younger trends between Anomaly 21 and Anomaly 18 because they are

sparse and widely spaced. Also, the cessation of motion between the Antarctic and Bellingshausen plates just after Chron 25 can be correlated with the end of seafloor spreading in the Tasman Sea (Weissel and Hayes, 1977) and to an increase in spreading rate between Antarctica and Australia (Cande and Mutter, 1982).

Further to the east, the Pacific-Antarctic ridge jumped northward almost instantaneously from the Tula Fracture Zone (Cande et al., 1982) to just west of the Menard Fracture zone (Fig. 14, fracture zones identified on Fig. 2). When this happened, a piece of the Pacific plate created at the Pacific-Aluk spreading center was transferred to the Antarctic plate. Anomalies 21 through 27 now appear on the Antarctic plate south of the Humboldt Fracture Zone, whereas the northward-aging Anomalies 28 through 34 that were formed at the Aluk-Pacific boundary are still on the Pacific plate (Cande et al., 1982). The scars left from the new rift extending the Pacific-Antarctic ridge to the Farallon plate are the Henry Trough on the Pacific plate and the Hudson Trough on the Antarctic plate. Both the Henry Trough and the Hudson Trough can be clearly seen in the vertical deflection lineations (Fig. 5). In addition, the difference in spreading rate between the fast Pacific-Aluk spreading and slower Pacific-Antarctic is expressed in the Geosat data. To the north of the Henry Trough, the lineations are sparse, reflecting the fast spreading rate (15.6 mm/yr) of the Pacific-Aluk boundary; whereas to the south, the lineations are abundant, reflecting the slower spreading rate (5.0 mm/yr) on the Pacific-Antarctic boundary.

Prior to the major ridge reorganization at Chron 21, the Farallon plate had undergone a change in relative motion. The magnetic lineations of Cande et al. (1982) indicate that the Farallon plate began to rift away from the Pacific-Aluk spreading segment along the Humboldt Trough just prior to Anomaly 23 (54.0 Ma). The spreading center on this ridge, which is now the Chile Rise, had an orientation parallel to the Humboldt Trough, with a spreading direction perpendicular to the Humboldt Trough. The lineations created at this ridge are now preserved on the Antarctic plate to the north of the Humboldt Trough. As Cande et al. (1982) pointed out, the spreading center

parallel to the Humboldt Trough became active before the Pacific-Antarctic plate boundary cut off the segment of crust that had been created at the Pacific-Aluk spreading south of the Humboldt Fracture Zone. Therefore, identified anomalies north of the Humboldt Fracture Zone between Anomaly 23 and Anomaly 21 were created on the Pacific-Farallon boundary, and Anomaly 21 and younger of the same sequence were created at the Antarctic-Farallon boundary.

D. EOCENE TO OLIGOCENE: CHRON 18 TO CHRON 7 (42.0 - 25.8 Ma)

The plate boundaries were fairly stable in the South Pacific region between Anomaly 18 and Anomaly 7 (42.0 Ma to 25.8 Ma) (Figs. 15 to 18). Spreading on the Pacific-Antarctic boundary occurred at an average rate of 27 mm/yr throughout the period. The azimuth for spreading gradually changed from an orientation of N30°W to N55°W along the Pacific-Antarctic Ridge. As a result of this change in orientation, the Eltanin Fracture Zone system narrowed, and the ridge segment between the Heezen and Tharp fracture zones shortened.

Along the Pacific-Farallon spreading center, the direction of spreading was constant, as is reflected in the interpretation of the Geosat data for the Pacific plate. The spreading rates we calculated using our spreading directions show a change from around 40 mm/yr prior to the time of Anomaly 18 to a rate of 150 m/yr between Anomaly 13 and 18. This very fast rate is close to the spreading rate observed on the EPR at the present time.

During the time period between Chron 18 and Chron 7, the Antarctic-Farallon spreading center rotated from a orientation of N60°W to an orientation of N20°W as new crust was accreted to the Antarctic plate. The Pacific-Antarctic-Farallon triple junction, which we model as a RRR type, moved rapidly 600 km to the northwest. The old Pacific-Aluk spreading center became the Antarctic-Aluk spreading center when the Pacific-Antarctic spreading center cut through to the Farallon plate at the time of Anomaly 21. Between the Tula and Hero fracture zones, the ridge collided with the West Antarctic Peninsula just after Chron 6 (19.35 Ma) (Barker, 1982). This

collision is analogous to the collision of the older ridge segment with Thurston Island south of the Hero Fracture Zone more than 50 million years ago.

E. OLIGOCENE TO MIOCENE: CHRON 7 TO CHRON 5 (25.8 - 10.6 Ma)

Between Chron 7 (Fig. 18) and Chron 5 (Fig. 19), major changes in plate motion took place in the South Pacific. The most important change occurred along the Pacific-Farallon spreading center. The Farallon plate broke up into two plates: the Cocos plate to the north and the Nazca plate to the south (Herron and Heirtzler, 1967; Raff, 1968). Between 10 and 20 million years ago, spreading between these two new plates initiated along the Galapagos Rise. At about the same time, spreading along the East Pacific Rise was reoriented from a northeasterly direction to a northwesterly direction. During the very earliest history of the EPR, a dual spreading center existed. South of the Galapagos Spreading Center on the Nazca plate is a linear feature on the ocean floor with an anomalously shallow depth. Herron (1972) and Anderson and Sclater (1972) named this feature the Galapagos Rise and sketch the trend of the feature to be northwesterly. Mammerickx et al. (1980) further investigated this feature, and identified the true trend as being parallel to the present EPR. After the change in orientation occurred, the EPR began spreading along what is now the Galapagos Rise. Shortly before Chron 5 (10.6 Ma), a new spreading center formed to the west. At that time, spreading occurred on both the Galapagos Rise and the present-day East Pacific Rise in a situation analogous to spreading on the Easter Microplate today (Handschumacher et al., 1981). Seafloor spreading along the Galapagos Rise stopped at about Chron 4 (6.5 Ma).

The changes in spreading direction in the southern South Pacific were related to major changes to the north. The Pacific-Antarctic Rise experienced a increase of the spreading rate from around 30 mm/yr to about 50 mm/yr on the northern part of the ridge. The Chile Rise also underwent a major change in orientation from a northwesterly orientation to a more north-south orientation

(Cande et al., 1982). The Pacific-Nazca-Antarctic triple junction changed from a RRR to a RFF type.

The triple junction between the South American, Nazca and Antarctic plates lies just off the South American coast at 46°S. It is presently a RTT type triple junction (Cande and Leslie, 1986). Since the beginning of the collision of Chile Ridge with the Chile Trench between 14 and 10 Ma, a history of complex interactions can be seen in both the seafloor morphology and geological features on land.

F. PLIOCENE to RECENT: ANOMALY 3 - PRESENT (4.7 - 0 Ma)

During the past 5 million years, the Pacific region has been relatively stable (Figs. 1 and 20). The most notable change in the region has been the development of the Easter and Juan Fernandez Microplates along the southern EPR. The Easter Microplate came into existence at about the time of Anomaly 2, when a new spreading center (Este) developed to the east of the main ridge (Oeste) (Handschumacher et al., 1981). The Juan Fernandez Microplate is a small plate which exists at the Pacific-Antarctic-Nazca triple junction (Anderson-Fontana et al., 1986).

Between the Shackleton Fracture Zone and the Hero Fracture Zone further to the south and to the west may be a remnant of the old Aluk plate, the Drake plate (Barker, 1982). A fossil spreading center separated the Antarctic crust to the north from the Drake plate (Fig. 2). Most of the Aluk plate has been subducted beneath the West Antarctic Peninsula margin (Cande et al., 1982), and extension continues in the Bransfield Strait. The youngest identifiable magnetic anomalies along the extinct Antarctic-Drake boundary are 4 to 5 million years old (Barker, 1982).

IMPLICATIONS FOR THE TECTONIC HISTORY OF THE NEW ZEALAND AND ROSS SEA REGIONS

New Zealand is a complicated zone of plate motion. The plate boundary between the Pacific

and Indo-Australian plates trends along Macquarie Ridge and the Alpine Fault, then connects with the boundary between the Pacific plate and the marginal basins to the west. The Indo-Australian plate is being subducted beneath the Pacific plate in the Hjort Trench and the Puysegur Trough, two of the features which make up the Macquarie Ridge complex (Kamp, 1986). The Alpine Fault separates the eastern part of South Island, which is on the Pacific plate, from the western section of South Island and North Island, which are on the Indo-Australian plate. Movement along the Alpine Fault is in a right-lateral sense with oblique convergence (Weissel et al., 1977). According to Falconer (1972), the slip rate along the fault is 35 mm/yr. Our calculations using the poles from present-day motion models of Minster and Jordan (1978) and Chase (1978) indicate a slip rate closer to 46 mm/yr. The direction of plate motion calculated from their poles is approximately east-west, confirming a transpressional environment on the northeast-trending fault.

There are two orogenic episodes in New Zealand which are difficult to resolve (Kamp, 1987). Thus, it has been difficult to define geologically the date when motion along the Alpine Fault began. One phase of deformation, the Kaikoura orogeny, is associated with recent movement along the Alpine Fault and uplift of the Southern Alps. The other deformational event is related to the subduction of Pacific crust and accretion of the a series of exotic terranes along a trench system along the Pacific margin of Gondwanaland during the Mesozoic. This is the Rangitata Orogeny (Kamp, 1987). According to Kamp (1987), faulting associated with Pacific-Indo-Australian plate motion began at 23 Ma, with a cumulative slip of 480 km. Our reconstructions indicate that there was a total slip of approximately 550 km along the fault beginning sometime between Chron 7 (25.9 Ma) and present. This is in agreement with the figures of Kamp (1987). On the northern end of South Island, motion between the Pacific and Indo-Australian plates has been taken up in a complex, 100 km wide, brittle-ductile shear zone, the Marlborough Fault Zone. The plate boundary then passes to the east of North Island, where the Pacific plate is being subducted beneath the Indo-Australian plate in the Hikurangi Trough. This feature then connects with the

Tonga-Kermadec trench system.

The last deformational phase of the Rangitata Orogeny was Late Cretaceous (Kamp, 1987). We used this time as the time of cessation of subduction of Pacific crust under the Chatham Rise and New Zealand. This would mean that subduction stopped when the rifting of the Chatham Rise began.

DISCUSSION AND CONCLUSIONS

We conclude from our study that the use of geoid data, in conjunction with shipboard data, improves our ability to study the past positions of plates relative to each other and can help us understand in more detail the way that plates move with respect to each other. This is especially important in areas such as the South Pacific which have large areas which are difficult to access by ship. Our presentation of the Geosat data as plots of slope of the geoid (deflection of the vertical) versus satellite tracks has improved the amount of detail over the gridded approach of Haxby (1987). Because the flowlines which we can trace in the Geosat data are well-correlated with bathymetric identifications of fracture zones, these lineations in the vertical deflection charts can be used for plate reconstructions just as bathymetric lineations have been used in the past. The satellite altimetry data represent an improvement over the bathymetric identifications because they are more uniformly sampled. Using our vertical deflection lineations along with bathymetric lineations and a compilation of published magnetic anomaly identifications and magnetic lineations, we have constructed a tectonic fabric map of the South Pacific region. We used the features on the tectonic fabric map to calculate paleogeographic reconstructions for the Cenozoic and Late Cretaceous.

The past positions of the spreading centers from our reconstructions are compiled into an isochron chart of the South Pacific (Fig. 21). The fracture zones along the ridges are drawn parallel to the lineations in the vertical deflection charts and to small circles about the stage poles.

Therefore, the fracture zones do not appear as continuous features in the isochron chart.

There are several interesting features on the isochron chart. First, our study predicts that the oldest crust on the Nazca plate is older than Anomaly 34 (84.0 Ma). Second, there is still no prediction for the age of the oldest crust on the Cocos plate. Third, we have been able to successfully model the changes in distance between the Heezen and Tharp Fracture Zones by examining the changes in relative motion between the Pacific and Antarctic plates. The fracture zones drawn according to the small circles generated from our stage poles indicate that at around Chron 10, the spreading on the Pacific-Antarctic Ridge became briefly more east-west oriented than it was before or after, and this caused the length of the ridge segment between the two fracture zones to decrease for a short period of time.

Our study has raised several questions which need further study in the South Pacific. The most important problem yet to be resolved is that the Galapagos Spreading Center cannot be reconstructed according to plate tectonic theory at this time. We feel that our reconstructions are very well constrained on the northern part of the EPR by the magnetic anomaly identifications of Klitgord and Mammerickx (1982) and by our interpretation of the lineations in the vertical deflection charts. The southern limb of the EPR is much less well constrained by magnetic anomaly identifications; however, with good poles of rotation for Nazca-Antarctic and Antarctic-Pacific, we can calculate poles for Pacific-Nazca rotation along the southern EPR. Using these poles for the northern and southern EPR, we are unable to model reasonably the motion between the Nazca and Cocos plates. In addition, the age of the crust to the west of the Middle America trench on the Cocos plate remains unknown.

The southern EPR from the Pacific-Nazca-Cocos triple junction to the Pacific-Nazca-Antarctic triple junction needs to be restudied, and the magnetic anomalies re-identified. Also, along the older northwesterly-trending segment of the Pacific-Farallon spreading center north of 30°S, the magnetic anomaly identifications must be re-examined. A possible method for doing this could be

based upon extrapolating the identifications of Cande et al. (1982) northward and using the lineations in the vertical deflection charts as a guide for spreading direction.

In the central South Pacific, there is a problem regarding the Easter plate. If it is assumed that the Pacific plate and the Nazca plate behave as rigid plates, and that they are spreading apart along the EPR both north and south of the Easter plate, then the Anomaly 3 isochron cannot be drawn such that is does not overlap on the Anomaly 2 identifications by Handschumacher et al. (1981), either on the eastern side of Este, the new eastern spreading center, or the western side of Oeste, the western spreading center. There is simply too much crust, as identified by Handschumacher et al. (1981), to fit into the space between the two larger plates.

In the south, the age and structure of the crust north of Marie Byrd Land remains a mystery. The calculations of Stock and Molnar (1987) indicate the existence of a plate boundary in this region. Since this area is covered year-round with ice and lies south of the geoid satellite coverage area, it will be difficult to determine the age of this area of the Antarctic plate and explore the conjugate of the only passive margin in the South Pacific region.

A history of the crust to the north and east of the Anomaly 34 identifications of Cande et al. (1982) and west of the Tonga-Kermadec trench needs to be developed. Much of this area lies within the Cretaceous Quiet Zone; however, the morphology of the sea floor might yield clues to the history of this area.

There are several important times in the history of the South Pacific. The Chatham Rise split off from the Campbell Plateau and Marie Byrd Land prior to 84 Ma, opening up the Bounty Trough (Davey, 1977). Opening in the Bounty Trough then ceased, and spreading initiated between the Campbell Plateau and Marie Byrd Land at approximately 84 Ma. In the southwest Pacific, crust was being generated at two separate spreading centers between Chron 34 and Chron 25, one operating between Marie Byrd Land and the Pacific plate, and the other to the north separating the Pacific plate from the Bellingshausen plate. There was probably very slow

spreading on a boundary separating Marie Byrd Land (West Antarctic plate) and the Bellingshausen plate.

Between Chron 25 and Chron 21 (58.9 - 49.6 Ma) (Figs. 13 and 14), spreading ceased on the Bellingshausen-West Antarctic plate boundary. A part of the crust generated at the Pacific-Aluk spreading center was cut off and trapped on the Antarctic plate. The new Pacific-Antarctic Rise began opening about the same pole from the Farallon-Antarctic-Pacific triple junction to the Macquarie Ridge. The Pacific-Farallon spreading center became slightly reoriented to a more north-south trend. These changes happened at roughly the same time that the spreading ceased in the Tasman Sea (Weissel and Hayes, 1977).

The next major change in the South Pacific occurred between Chron 7 and Chron 5 (25.8 - 10.6 Ma). The Farallon plate split into the Nazca and Cocos plates. At the same time, the East Pacific Rise became reoriented from a northwesterly direction to a northeasterly direction. The southern end of the Chile Rise collided with the coast of South America and became gradually reoriented from a northwest-southeast trend to an almost north-south trend (Cande et al., 1982). Also, the segment of the Antarctic-Aluk spreading center between the Tula and Hero fracture zones collided with the West Antarctic Peninsula.

ACKNOWLEDGEMENTS

This paper was originally written as a thesis by Catherine L. Mayes at the University of Texas at Austin under the supervision of John Sclater. We would thank Ian Dalziel, Christoph Huebeck and Dale Sawyer for reviewing the paper. We would also like to thank Joann Stock for her careful and helpful review of the reconstructions and poles of rotation. This work was supported by the Shell Professorship granted to John Sclater, the Paleoceanographic Mapping Project, and a Teaching Assistantship in the Department of Geological Sciences at the University of Texas at Austin, and by the NASA Geodynamics Program (NAG5-787).

References

Anderson, R. N., and Sclater, J. G., Evolution of the East Pacific Rise, Earth Planet. Sci. Lett., 14, 433-441, 1972.

Anderson-Fontana, S., Engeln, J. F., Lundgren, P., Larson, R. L., and Stein, S., Tectonics and evolution of the Juan Fernandez microplate at the Pacific-Nazca-Antarctic triple junction, J. Geophys. Res., 91(B2), 2005-2018, 1986.

Barker, P. F., The Cenozoic subduction history of the Pacific margin of the Antarctic Peninsula: ridge crest - trench interactions, J. Geol. Soc. London, 139, 787-801, 1982.

Berggren, W. A., Kent, D. V., Flynn, J. J., and Van Couvering, J. A., Cenozoic geochronology, Geol. Soc. Am. Bull., 96(11), 1407-1418, 1985.

Bonatti, E., Harrison, C. G. A., Fisher, D. E., Honnorez, J., Schilling, J.-G., Stipp, J. J., and Zentilli, M., Easter volcanic chain (Southeast Pacific): a mantle hot line, J. Geophys. Res., 82, 2457-2478, 1977.

Burns, R. E., Andrews, J. E., et al., Site 207, *in* Burns, R. E., and Andrews, J. E., et al. (eds.), Initial Reports of the Deep Sea Drilling Project, Vol. 21, Washington: U.S. Government Printing Office, 197-269, 1973.

Cande, S. C., Herron, E. M., and Hall, B. R., The early Cenozoic history of the southeast Pacific, Earth Planet. Sci.Lett., 57, 63-74, 1982.

Cande, S. C., LaBrecque, J. L., and Haxby, W. B., Plate kinematics of the South Atlantic: chron 34 to present, J. Geophys. Res., in press.

Cande, S. C., and Leslie, R. B., Late Cenozoic tectonics of the southern Chile Trench, J. Geophys. Res., 91(B1), 471-496, 1986.

Cande, S. C., and Mutter, J., A revised interpretation of the oldest sea floor spreading anomalies between Australia and Antarctica, Earth Planet. Sci. Lett., 58, 151-160, 1982.

Chase, G. C., Plate kinematics: the Americas, East Africa, and the rest of the world, Earth Planet. Sci. Lett., 37, 355-368, 1978.

Christoffel, D. A., and Falconer, R. H. H., Marine magnetic measurements in the southwest Pacific Ocean and the identification of new tectonic features, *in* Antarctic Oceanology II - The Australian-New Zealand Sector, D. E. Hayes (ed.), 197-209, Washington: AGU, 1972.

Craig, C. H., and Sandwell, D. T., The global distribution of seamounts from SEASAT profiles, J. Geophys. Res., in press.

Crook, K. A. W., and Belbin, L., The Southwest Pacific area during the last 90

million years, J. Geol. Soc. Aust., 25(1), 23-40, 1978.

Davey, F. J., Marine seismic measurements in the New Zealand Region, N. Z. J. Geol. and Geophys., 20(4), 719-777, 1977.

Drewry, D. J., and Jordan, S. R., "Bedrock surface of Antarctica", Sheet 3 of Antarctica: Glaciological and Geophysical Folio, Drewry, D. J. (ed.), Scott Polar Research Institute: Cambridge, 1983.

Falconer, R. K. H., The Indian-Antarctic-Pacific triple junction, Earth Planet. Sci. Lett., 17, 151-158, 1972.

Falconer, R. K. H., and Tharp, M., GEBCO Panel 5.14, IHO/IOC/CHS, GEBCO - General Bathymetric Chart Of The Oceans (5th Edition), International Hydrographic Organization / Intergovernmental Oceanic Commission / Canadian Hydrographic Service: Ottawa, Canada, 1984.

Grindley, G. W., and Davey, F. J., The reconstruction of New Zealand, Australia, and Antarctica, *in* Craddock, C. (ed.), Antarctic Geoscience, Madison: University of Wisconsin Press, 15-29, 1982.

Grunow, A. M., Kent, D. V., and Dalziel, I. W. D., Mesozoic evolution of West Antarctica and the Weddell Sea Basin: new paleomagnetic constraints, Earth Planet. Sci. Lett., 86, 16-26, 1987.

Handschumacher, D. W., Post-Eocene plate tectonics of the Eastern Pacific, *in* The Geophysics of the Pacific Ocean Basin and its Margins, AGU Monograph 19, G. H. Sutton et al. (ed.), Washington: AGU, 177-202, 1976.

Handschumacher, D. W., Pilger, R. H. Jr., Foreman, J. A., and Campbell, J. F., Structure and evolution of the Easter plate, *in* Geol. Soc. Am. Memoir 154, 63-76, 1981.

Hayes, D. E., and Ringis, J., Sea-floor spreading in the Tasman Sea, Nature, 454-458, 1973.

Haxby, W. F., Gravity field of the world's oceans, NOAA Report MGG-3, 1987.

Herron, E. M., Sea-floor spreading and the Cenozoic history of the east-central Pacific, Geol. Soc. Am. Bull., 83, 1671-1692, 1972.

Herron, E. M., and Heirtzler, J. R., Sea-floor spreading near the Galapagos, Science, 158, 775-780, 1967.

Herron, E. M., and Tucholke, B. E., Sea-floor magnetic patterns and basement structure in the southeastern Pacific, *in* Hollister, C. D., Craddock, C., et al. (eds.), Initial Reports of the Deep Sea Drilling Project, Vol. 35, Washington: U.S. Government Printing Office, 263-278, 1976.

Hey, R., Tectonic evolution of the Cocos-Nazca spreading center, Geol. Soc. Am.

Bull., 88, 1404-1420, 1977.

Johnson, G. L., and Vanney, J.-R., GEBCO Panel 5.18, IHO/IOC/CHS, GEBCO - General Bathymetric Chart Of The Oceans (5th Edition), International Hydrographic Organization / Intergovernmental Oceanic Commission / Canadian Hydrographic Service: Ottawa, Canada, 1984.

Kamp, P. J. J., Late Cretaceous-Cenozoic tectonic development of the southwest Pacific region, Tectonophysics, 121, 225-251, 1986.

Kamp, P. J. J., Age and origin of the New Zealand orocline in relation to Alpine Fault movement, J. Geol. Soc., London, 144, 641-652, 1987.

Karig, D. E., Ridges and basins of the Tonga-Kermadec Island Arc system, J. Geophys. Res., 75(2), 239-254, 1970.

Kent, D. V., and Gradstein, F. M. A., Cretaceous and Jurassic geochronology, Geol. Soc. Am. Bull., 96(11), 1419-1427, 1985.

Klitgord, K. D., and Lonsdale, P., Structure and tectonic history of the eastern Panama Basin, Geol. Soc. Am. Bull., 89, 981-999, 1978.

Klitgord, K. D., and Mammerickx, J., Northern East Pacific Rise: Magnetic anomaly and bathymetric framework, J. Geophys. Res., 6725-6750, 1982.

Klitgord, K. D., and Schouten, H., Plate kinematics of the central Atlantic, *in* The Western North Atlantic Region, The Geology of North America, Volume M, Vogt, P. R., and Tucholke, B. E. (ed.), Geol. Soc. Am.: Boulder, 351-378, 1986.

Lanphere, M., and Dalrymple, G. B., K-Ar ages of basalts from DSDP Leg 33: Sites 315 (Line Islands) and 317 (Manihiki Plateau), *in* Schlanger, S. O., Jackson, E. D., et al. (eds.), Initial Reports of the Deep Sea Drilling Project, Vol. 33, Washington: U.S. Government Printing Office, 649-654, 1976.

Larson, R. L., Late Jurassic and Early Cretaceous evolution of the Western Central Pacific Ocean, J. Geomag. Geoelectr., 28, 219-236, 1976.

Lawver, L. A., Sclater, J. G., and Meinke, L., Mesozoic and Cenozoic reconstructions of the South Atlantic, Tectonophysics, 114, 233-254, 1985.

MacArthur, J. L., Marsh Jr., P. C., and Wall, J. G., The GEOSAT radar altimeter, John Hopkins APL Technical Digest, 8, 176-181, 1987.

Mammerickx, J., Depth anomalies in the Pacific: Active, fossil and precursor, Earth Planet. Sci. Lett., 53, 147-157, 1981.

Mammerickx, J., Herron, E. M., Dorman, L., Evidence for two fossil spreading ridges in the southeast Pacific, Geol. Soc. Am. Bull., 91, 263-271,1980.

Mammerickx, J., and Sandwell, D. T., Rifting of old oceanic lithosphere, J. Geophys. Res., 92(B2), 1975-1988, 1986.

Mammerickx, J., and Smith, S. M., GEBCO Panel 5.7, IHO/IOC/CHS, GEBCO - General Bathymetric Chart Of The Oceans (5th Edition), International Hydrographic Organization / Intergovernmental Oceanic Commission / Canadian Hydrographic Service: Ottawa, Canada, 1984a.

Mammerickx, J., and Smith, S. M., GEBCO Panel 5.11, IHO/IOC/CHS, GEBCO - General Bathymetric Chart Of The Oceans (5th Edition), International Hydrographic Organization / Intergovernmental Oceanic Commission / Canadian Hydrographic Service: Ottawa, Canada, 1984b.

Mammerickx, J., Taylor, I. L., and Cande, S., GEBCO Panel 5.15, IHO/IOC/CHS, GEBCO - General Bathymetric Chart Of The Oceans (5th Edition), International Hydrographic Organization / Intergovernmental Oceanic Commission / Canadian Hydrographic Service: Ottawa, Canada, 1984.

Marsh, J. G., and Martin, T. V., The SEASAT altimeter mean sea surface model., J. Geophys. Res., 87, 3269-3280, 1982.

McConathy, D. R., and Kilgus, J. J., The Navy Geosat Mission: An Overview, Johns Hopkins APL Technical Digest, 8(2), 170-175,1987.

McNulty, C. L., Cretaceous foraminiferal stratigraphy, DSDP Leg 33, Sites 315A, 316, 317A *in* Schlanger, S. O., Jackson, E. D., et al. (eds.), Initial Reports of the Deep Sea Drilling Project, Vol. 33, Washington: U.S. Government Printing Office, 649-654, 1976.

Menard, H. W., The East Pacific Rise, Science, 132, 1737-1746, 1960.

Menard, H. W., Fracture zones and offsets of the East Pacific Rise, J. Geophys. Res., 71, 682-685, 1966.

Minster, J. B., and Jordan, T. H., Present-day plate motions, J. Geophys. Res., 83, 5331-5351, 1978.

Molnar, P., Atwater, T., Mammerickx, J., and Smith, S. M., Magnetic anomalies, bathymetry and the tectonic evolution of the South Pacific since the Late Cretaceous, Geophys. J. R. Astron. Soc., 40, 383-420, 1975.

Monahan, D., Falconer, R. K. H., and Tharp, M., GEBCO Panel 5.10, IHO/IOC/CHS, GEBCO - General Bathymetric Chart Of The Oceans (5th Edition), International Hydrographic Organization / Intergovernmental Oceanic Commission / Canadian Hydrographic Service: Ottawa, Canada, 1984.

Okal, E. A., and Cazenave, A., A model for the plate tectonic evolution of the east-central Pacific based on SEASAT investigations, Earth Planet. Sci. Lett., 72, 99-116, 1985.

Pardo-Casas, F., and Molnar, P., Relative motion of the Nazca (Farallon) and South American plates since Late Cretaceous time, Tectonics, 6(3), 215-232, 1987.

Patriat, P. L., Evolution du systme de dorsales de l'Ocean Indien, These Doctorat d'Etat, unpublished, Universite Pierre et Marie Curie, Paris, 1983.

Pitman, W. C., III, Herron, E. M., and Heirtzler, J. R., Magnetic anomalies in the Pacific and sea floor spreading, J. Geophys. Res., 73(6), 2069-2085, 1968.

Rabinowitz, P. D., and LaBrecque, J. L., The Mesozoic South Atlantic Ocean and evolution of its continental margins, J. Geophys. Res., 84, 5973-6002, 1979.

Raff, A. D., Sea-floor spreading - another rift, J. Geophys. Res., 73, 3699-3705, 1968.

Rosa, J. W. C., and Molnar, P., Uncertainties in reconstructions of the Pacific, Farallon, Vancouver and Kula plates and constraints on the rigidity of the Pacific and Farallon (and Vancouver) plates between 72 and 35 Ma, J. Geophys. Res., 93(B4), 2997-3008, 1988.

Ross, M. I., and Scotese, C. R., Hierarchical tectonic analysis of the Gulf of Mexico and Caribbean Region, Tectonophysics, in press.

Sailor, R. V., and Okal, E. A., Applications of SEASAT altimeter data in seismotectonic studies of the South-Central Pacific, J. Geophys. Res., 88, 1572-1580, 1983.

Sandwell, D. T., and McAdoo, D. C., Marine gravity of the Southern Ocean and Antarctic margin from GEOSAT, J. Geophys. Res., in press.

Sandwell, D. T., and Schubert, G., Geoid and height-age relation from SEASAT altimeter profiles across the Mendocino Fracture Zone, J. Geophys. Res., 87, 3949-3958, 1982.

Sclater, J. G., Anderson, R. N., and Bell, M. L., Elevation of ridges and evolution of the central eastern Pacific, J. Geophys. Res., 76, 7888-7915, 1971.

Scotese, C. R., Gahagan, L. M., and Larson, R. L., Plate tectonic reconstructions of the Cretaceous and Cenozoic ocean basins, Tectonophysics, in press.

Scotese, C. R., Ross, M. I., Lottes, A. L., and Bennett, C., Plate tectonic modelling using interactive computer graphics, Tectonophysics, in press.

Shaw, P. R., and Cande, S. C., Shape and amplitude analysis of small-offset fracture zone geoid signals, EOS, 68 (44), 1462, 1987.

Stock, J., and Molnar, P., Uncertainties in the relative positions of the Australia, Antarctica, Lord Howe and Pacific plates since the Late Cretaceous, J. Geophys. Res., 87 (B6), 1982.

Stock, J., and Molnar, P., Revised history of early Tertiary plate motion in the south-west Pacific, Nature, 325, 495-499, 1987.

Storey, B. C., Grunow, A. M., Dalziel, I. W. D., Pankhurst, R. J., and Millar, I., A new look at the geology of Thurston Island (abstract), 5th International Symposium on Antarctic Earth Sciences, Cambridge, 123, 1987.

Tapley, B. D., Born, G. H., and Parke, M. E., The SEASAT altimeter data and its accuracy assessment, J. Geophys. Res., 87, 3179-3188, 1982.

Weissel, J. K., and Hayes, D. E., Evolution of the Tasman Sea reappraised, Earth Planet. Sci. Lett., 36, 77-84, 1977.

Weissel, J. K., Hayes, D. E., and Herron, E. M., Plate tectonics synthesis: the displacements between Australia, New Zealand and Antarctica since the Late Cretaceous, Marine Geology, 25, 231-277, 1977.

Winterer, E. L., Bathymetry and regional tectonic setting of the Line Islands Chain, *in* Schlanger, S. O., Jackson, E. D., et al. (eds.), Initial Reports of the Deep Sea Drilling Project, Vol. 33, Washington: U. S. Government Printing Office, 731-747, 1976.

Table 1 - Ages Assigned to Reconstructions and Mangetic anomalies
Based on Berggren et al., 1985

Anomaly	Time (Ma)
0	0.0
3	4.7
5	10.6
7	25.8
10	30.0
13	35.7
18	42.0
21	49.6
25	58.9
28	64.3
31	69.0
34	84.0

Table 2 -Finite Poles of Rotation

SOUTH AMERICA TO AFRICA

Anom.	Time	Lat.	Long.	Angle	Reference
0	0.0	0.00	0.00	0.00	PRESENT
6	20.0	59.00	-35.00	7.70	LAWVER ET AL. 1985
13	35.5	59.00	-35.00	13.70	LAWVER ET AL. 1985
28	64.0	63.00	-36.00	24.30	LAWVER ET AL. 1985
34	84.0	63.00	-36.00	33.80	LAWVER ET AL. 1985
M0	116.0	55.10	-35.70	50.90	LAWVER ET AL. 1985

AUSTRALIA TO ANTARCTICA

Anom.	Time	Lat.	Long.	Angle	Reference
0	0.0	0.00	0.00	0.00	
5	10.5	13.30	37.70	-6.62	ROYER, PERS. COMM.
6	20.5	14.50	32.80	-11.98	ROYER, PERS. COMM.
13	35.5	13.40	32.70	-20.40	ROYER, PERS. COMM.
18	42.0	16.60	29.90	-23.62	ROYER, PERS. COMM.
20	46.2	14.80	30.90	-24.33	ROYER, PERS. COMM.
24	56.1	13.80	30.50	-25.32	ROYER, PERS. COMM.
31	68.5	9.00	33.50	-25.83	ROYER, PERS. COMM.
33	80.2	6.20	35.00	-26.37	ROYER, PERS. COMM.
34	84.0	5.20	5.70	-26.85	ROYER, PERS. COMM.
	96.0	1.00	38.00	-28.30	ROYER, PERS.COMM.

EAST ANTACRTICA TO AFRICA

Anom.	Time	Lat.	Long.	Angle	Reference
0	0.0	0.00	0.00	0.00	
2	1.9	18.55	-36.41	0.33	SCOTESE ET AL. (IN PRESS)
3A	5.9	9.45	-41.72	0.82	SCOTESE ET AL. (IN PRESS)
5	10.6	8.50	-51.80	1.44	ROYER, PERS. COMM.
6	20.5	13.40	-55.10	2.79	ROYER, PERS. COMM.
8	27.7	13.60	-51.80	4.02	PATRIAT, 1983
15	37.7	8.73	-36.52	5.93	SCOTESE ET AL. (IN PRESS)
20	46.2	11.40	-43.70	7.81	ROYER, PERS. COMM.
21	49.6	10.30	-42.90	8.77	ROYER, PERS. COMM.
24	56.1	6.70	-40.60	9.97	ROYER, PERS. COMM.
26	60.8	3.80	-39.70	10.63	ROYER, PERS. COMM.
28o	64.3	0.60	-39.20	11.32	ROYER, PERS. COMM.
29	66.2	-0.40	-39.40	11.59	ROYER, PERS. COMM.
31o	68.4	1.10	-41.60	11.84	ROYER, PERS. COMM.
32	71.7	-1.80	-41.40	13.47	ROYER, PERS. COMM.
33	80.2	-4.70	-39.70	16.04	ROYER, PERS. COMM.
34	84.0	-2.00	-39.20	17.85	ROYER, PERS. COMM.

Table 2 -Finite Poles of Rotation (cont.)

WEDDELLIA TO EAST ANTARCTICA

Anom.	Time	Lat.	Long.	Angle	Reference
0	0.0	0.00	0.00	0.00	
34	84.0	14.82	-20.98	-5.90	THIS PAPER
	90.0	70.26	76.70	-10.48	THIS PAPER

NORTH NEW ZEALAND (LORD HOWE RISE) TO AUSTRALIA

Anom.	Time	Lat.	Long.	Angle	Reference
0	0.0	0.00	0.00	0.00	
25	60.0	0.00	0.00	0.00	WEISSEL AND HAYES 1977
26	65.0	-1.50	138.50	-2.55	WEISSEL AND HAYES 1977
29	69.0	-5.50	140.50	-6.60	WEISSEL AND HAYES 1977
32	75.0	-11.40	141.50	-12.75	WEISSEL AND HAYES 1977
33	82.0	-14.00	142.00	-19.00	WEISSEL AND HAYES 1977
FIT	90.0	-14.00	142.00	-23.00	WEISSEL AND HAYES 1977

CAMBPELL PLATEAU (SOUTH ISLAND OF NEW ZEALAND) TO PACIFIC

Anom.	Time	Lat.	Long.	Angle	Reference
0	0.0	0.00	0.00	0.00	
	245.0	0.00	0.00	0.00	CROOK AND BELBIN, 1978

CHATHAM RISE TO PACIFIC

Anom.	Time	Lat.	Long.	Angle	Reference
0	0.0	0.00	0.00	0.00	
32	74.0	0.00	0.00	0.00	
34	84.0	0.00	0.00	0.00	
FIT	90.0	-31.65	143.87	-4.21	CROOK AND BELBIN, 1978

BELLINGSHAUSEN PLATE TO PACIFIC

Anom.	Time	Lat.	Long.	Angle	Reference
0	0.0	0.00	0.00	0.00	
25	58.9	71.81	-60.67	-39.39	THIS PAPER
28	64.3	70.77	-58.37	-45.52	THIS PAPER
31	69.0	70.31	-56.34	-50.92	THIS PAPER

PACIFIC TO MARIE BYRD LAND (WEDDELLIA)

Anom.	Time	Lat.	Long.	Angle	Reference
0	0.0	0.00	0.00	0.00	
3	4.7	66.20	-83.50	4.13	THIS PAPER
5	10.6	70.44	-78.84	9.12	THIS PAPER
7	25.8	73.13	-72.44	19.52	THIS PAPER
10	30.0	73.73	-69.54	22.52	THIS PAPER
13	35.7	73.67	-65.98	26.68	THIS PAPER
18	42.0	72.78	-64.61	29.89	THIS PAPER
21	49.6	72.09	-63.44	33.93	THIS PAPER

Table 2 -Finite Poles of Rotation (cont.)

PACIFIC TO MARIE BYRD LAND (WEDDELLIA)

Anom.	Time	Lat.	Long.	Angle	Reference
25	58.9	70.32	-63.45	36.77	THIS PAPER
28	64.3	68.69	-63.47	39.88	THIS PAPER
31	69.0	67.12	-63.02	44.53	THIS PAPER
34	84.0	64.94	-62.49	53.09	THIS PAPER
	90.0	64.03	-56.96	57.65	THIS PAPER

NAZCA TO PACIFIC

Anom.	Time	Lat.	Long.	Angle	Reference
0	0.00	0.00	0.00	0.00	
3	4.7	58.86	-89.43	-6.60	THIS PAPER
5	10.6	60.13	-89.76	-15.18	THIS PAPER
7	25.8	65.41	-92.00	-39.35	THIS PAPER
10	30.0	66.20	-98.41	-44.05	THIS PAPER
13	35.7	69.04	-104.34	-49.63	THIS PAPER
18	42.0	71.68	-113.62	-56.17	THIS PAPER
21	49.6	72.45	-117.31	-58.80	THIS PAPER
25	58.9	73.47	-123.51	-63.31	THIS PAPER
28	64.3	73.94	-127.15	-66.04	THIS PAPER
31	69.0	74.24	-129.95	-68.20	THIS PAPER
34	84.0	74.81	-137.06	-73.96	THIS PAPER

COCOS TO PACIFIC

Anom.	Time	Lat.	Long.	Angle	Reference
0	0.0	0.00	0.00	0.00	
3	4.7	31.62	-106.80	-10.64	THIS PAPER
5	10.6	47.13	-106.64	18.57	THIS PAPER

Figure Captions

Fig. 1a : Bathymetry (in meters) and major features of the South Pacific region (from mini-GEBCO, version 5.0).

Fig. 1b : Bathymetry (in meters) and major features of the Pacific margin of Antarctica (from mini-GEBCO, version 5.0).

Fig. 2 : Compilation of magnetic picks and lineations and fracture zones for the South Pacific. Sources include: Klitgord and Mammerickx, 1982; Herron, 1972; Handschumacher, 1976; Pardo-Casas and Molnar, 1987; Mammerickx et al., 1980; Handschumacher et al., 1981; Cande et al., 1983; Larson, 1976; Herron and Tucholke, 1976; Barker, 1983; Molnar et al., 1975; Weissel and Hayes, 1977; Christoffel and Falconer, 1972.

Fig. 3a : Deflection of the vertical, plotted perpendicular to track, descending passes, in the South Pacific. Present-day spreading centers are drawn with a light black line. Small dots mark earthquake locations (Bulletin of the International Seismological Centre).

Fig. 3b : Deflection of the vertical plotted perpendicular to track, ascending passes, in the South Pacific. Present-day spreading centers are drawn with a light black line.

Fig. 4a : Resulting geoid anomaly and deflection of the vertical (slope of the geoid) signal for a seamount, trough, and fracture zone.

Fig. 4b : Deflection of the vertical over a fracture zone/transform fault in the vicinity of a ridge. Y = side of the transform or fracture zone on which crust is younger. O = side of transform fault or fracture zone where crust is older. A lineation drawn on a line of peaks on one side of the active ridge is matched with the lineation from a line of troughs on the other side of the ridge. The ridge position can be estimated by identifying the change in polarity along a fracture zone lineation.

Fig. 5 : Tectonic fabric lineations derived from the deflection of the vertical for the South Pacific. Symbols indicate ground track crossings. O = points of maximum positive slope (traveling from south to north). + = points of maximum negative slopes.

Fig. 6a : Comparison of vertical deflection and bathymetry over the northern portion of the Eltanin fracture zone system. Bathymetry from GEBCO chart 5.15 (Mammerickx et al., 1984) in 500 m intervals. Dotted lines are ship tracks. There is a close correspondence between the bathymetry and the vertical deflection lineations. We can therefore use the lineations we identify in the vertical deflection in the same way as we use fracture zone identifications to make plate reconstructions. In many cases, it is better to use the vertical deflection lineations because they are more uniformly sampled than the bathymetry from the ship tracks.

Fig. 6b : Comparison of deflection of the vertical and bathymetry over the central portion of the Eltanin fracture zone system.

Fig. 6c : Comparison of deflection of the vertical and bathymetry over the southern portion of the Eltanin fracture zone system.

Fig. 7 : Generalized tectonic fabric map of the South Pacific. Magnetic picks and lineations from published sources are combined with the tectonic fabric derived from the deflection of the vertical (solid lines). Where there are no good vertical deflection lineations, i.e. on the fast-spreading Pacific-Nazca plate boundary and on the small-offset fracture zones on the Galapagos Spreading Center, bathymetric identifications (dashed lines) have been included.

Fig. 8a: Spreading azimuths and half-rates calculated using the finite poles of rotation of the Antarctic (Bellingshausen) / Pacific plate pair at 42°S, 85°W on the northern segment of the Pacific-Antarctic Rise. Azimuths shown are directions of spreading on the Pacific plate. Azimuths are nearly east-west at present and gradually increase to 115° east.

Fig. 8b: Spreading rates and azimuths for the Antarctic (Weddellia) / Pacific plate pair at 65°S, 170°W on the southern portion of the Pacific-Antarctic Rise. Prior to Chron 21 (49.6 Ma), the Pacific and West Antarctica were opening about a different pole than the Pacific-Bellingshausen further north. Azimuths shown are on the Pacific plate. Azimuths along the Pacific / Marie Byrd Land spreading center are around S20°E. As the Pacific-Antarctic Rise starts spreading along one pole, the azimuths decrease to S50°E. Spreading rates show a corresponding change.

Fig 8c: Spreading azimuths and rates along the Pacific / Nazca (Farallon) boundary at 5°S, 105°W (solid lines) and 46°S, 112°W (dashed lines). Azimuths shown are on the Pacific plate. The spreading rate increases to 120 mm/yr at Chron 18 (42.0 Ma), but the azimuth does not begin to change until Chron 13. The major change in azimuth occurs between Chrons 7 and 5, at which time the spreading rate increases to 160 mm/yr.

Fig. 9 : Tectonic reconstruction for the Cretaceous Quiet Zone (90 Ma). Configuration before the break-up of the Campbell Plateau and the Chatham Rise off Marie Byrd Land. The Tasman Sea has been closed about a pole by Weissel and Hayes (1977). To maintain the relative positions of North and South Islands of New Zealand, the Ross Sea has been closed by about 40%. The spreading center is Anomaly M0 and is inferred by extrapolating backward from Anomaly 34. The Manihiki Plateau is dated at 120 Ma and is the approximate location of Anomaly M0. Continental margin of Antarctica is from 2000 m isobath from Drewry and Jordan (1983) and Johnson and Vanney (1984). Continental margin on Campbell Plateau interpreted from Geosat. The relative positions of East Antarctica and Weddellia were obtained only by deriving the relative positions of the two pieces of New Zealand. Pacific plate (Campbell Plateau) are held fixed in all reconstructions.

Fig. 10 : Tectonic reconstruction for Chron 34. In the southwest Pacific, spreading has begun between the Campbell Plateau and the Chatham Rise and Marie Byrd Land. Spreading is also occurring along the Pacific-Bellingshausen and Pacific-Aluk plate boundaries. Bounty Trough has opened, rifting the Chatham Rise away from the Campbell Plateau. Double line indicates active spreading centers; squares are anomaly identifications on the Pacific plate; circles are anomaly identifications on the

Antarctic plate; triangles are anomaly identifications on the Farallon (Nazca) plate. The relative positions of East Antarctica and Weddellia were obtained only by deriving the relative positions of the two pieces of New Zealand.

Fig. 11 : Tectonic reconstruction for Chron 31. Spreading has begun in the Tasman Sea, rifting the Lord Howe Rise away from Australia. The Ross Sea has opened to its present-day width. The Chatham Rise is attached to the Pacific plate. Apparent separation between the two parts of New Zealand is probably due to the accumulated error of the Pacific-Antarctica, Antarctica-Australia and Australia-Lord Howe Rise plate circuit. Symbols as in Fig. 9.

Fig 12 : Tectonic reconstruction for Chron 28. A dual spreading center is operating north of the Tharp Fracture Zone, accommodating rapid motion between the Pacific and Aluk plates. This dual system is propagating northward. Crust between the two spreading centers is attached to the Bellingshausen plate. The Tasman Sea continues to open. Movement along the Antarctic-Bellingshausen boundary is of unknown orientation. Apparent separation between the two parts of New Zealand is probably due to the accumulated error of the Pacific-Antarctica, Antarctica-Australia and Australia-Lord Howe Rise plate circuit. Symbols as in Fig. 9.

Fig. 13 : Tectonic reconstruction for Chron 25. The dual spreading centers in the southeast Pacific continue to separate. Motion in the Ross Sea also continues, but the Tasman Sea has reached its maximum opening at Chron 25. Apparent separation between the two parts of New Zealand is probably due to the accumulated error of the Pacific-Antarctica, Antarctica-Australia and Australia-Lord Howe Rise plate circuit. Symbols as in Fig. 9.

Fig. 14 : Tectonic reconstruction for Chron 21. Major changes have occurred in the plate configuration in the South Pacific. The Pacific-Antarctic Rise is now spreading about the same pole from the Macquarie Ridge to the Pacific-Antarctic-Farallon triple junction. Motion between Marie Byrd Land and the Bellingshausen plate has ceased. The Pacific-Antarctic Rise has broken through the older crust on the Pacific-Aluk spreading center, and transferred a piece of northward-aging crust created at the old spreading center to the Antarctic plate (Cande et al., 1982). The Farallon plate has begun to move in a more northerly direction relative to the Antarctic plate, creating Anomaly 23 - Anomaly 21 to the north of the Humboldt Trough. A segment of the Antarctic-Aluk spreading center has collided with the Antarctic margin in the vicinity of Alexander Island. Symbols as in Fig. 9.

Fig. 15 : Tectonic reconstruction for Chron 18. More crust is accreted to the Antarctic-Farallon boundary. Symbols as in Fig. 9.

Fig. 16 : Tectonic reconstruction for Chron 13. Spreading continues as at Chron 18. Another segment of the Antarctic-Aluk spreading center between the Heezen and Tula Fracture Zones has collided with the Antarctic margin (Barker, 1982). Subduction continues to occur north of Alexander Island. Apparent overlap in New Zealand is probably caused by accumulated error in the poles of rotation. Symbols as in Fig. 9.

Fig. 17 : Tectonic reconstruction for Chron 10. Spreading continues as at Chron 13. Symbols as in Fig. 9.

Fig. 18 : Tectonic reconstruction for Chron 7. Antarctic-Farallon spreading center is gradually reorienting itself to a more northerly direction. Symbols as in Fig. 9.

Fig. 19 : Tectonic reconstruction for Chron 5. The Farallon plate has broken into two plates, the Cocos and the Nazca plates and rifting initiated along the Galapagos Spreading Center. The Pacific-Farallon spreading center (now Pacific-Nazca and Pacific-Cocos) was reoriented from a northwesterly to a northeasterly orientation. This new East Pacific Rise is spreading along a dual spreading center, along both the East Pacific Rise and the Galapagos Rise. The Chile Rise has been reoriented to almost north-south spreading. Another ridge-trench collision along the Antarctic margin between the Tula and Hero Fracture Zones has occurred. Movement has begun on the Alpine Fault in New Zealand. Symbols as in Fig. 9.

Fig. 20 : Tectonic reconstruction for Chron 3. Spreading continues as at Chron 5. The Galapagos Rise is now a fossil spreading center on the Nazca plate. Motion continues on the Alpine fault. Symbols as in Fig. 9.

Fig 21 : Present-day. Isochron chart of the South Pacific generated using the locations of the old spreading centers from our reconstructions.

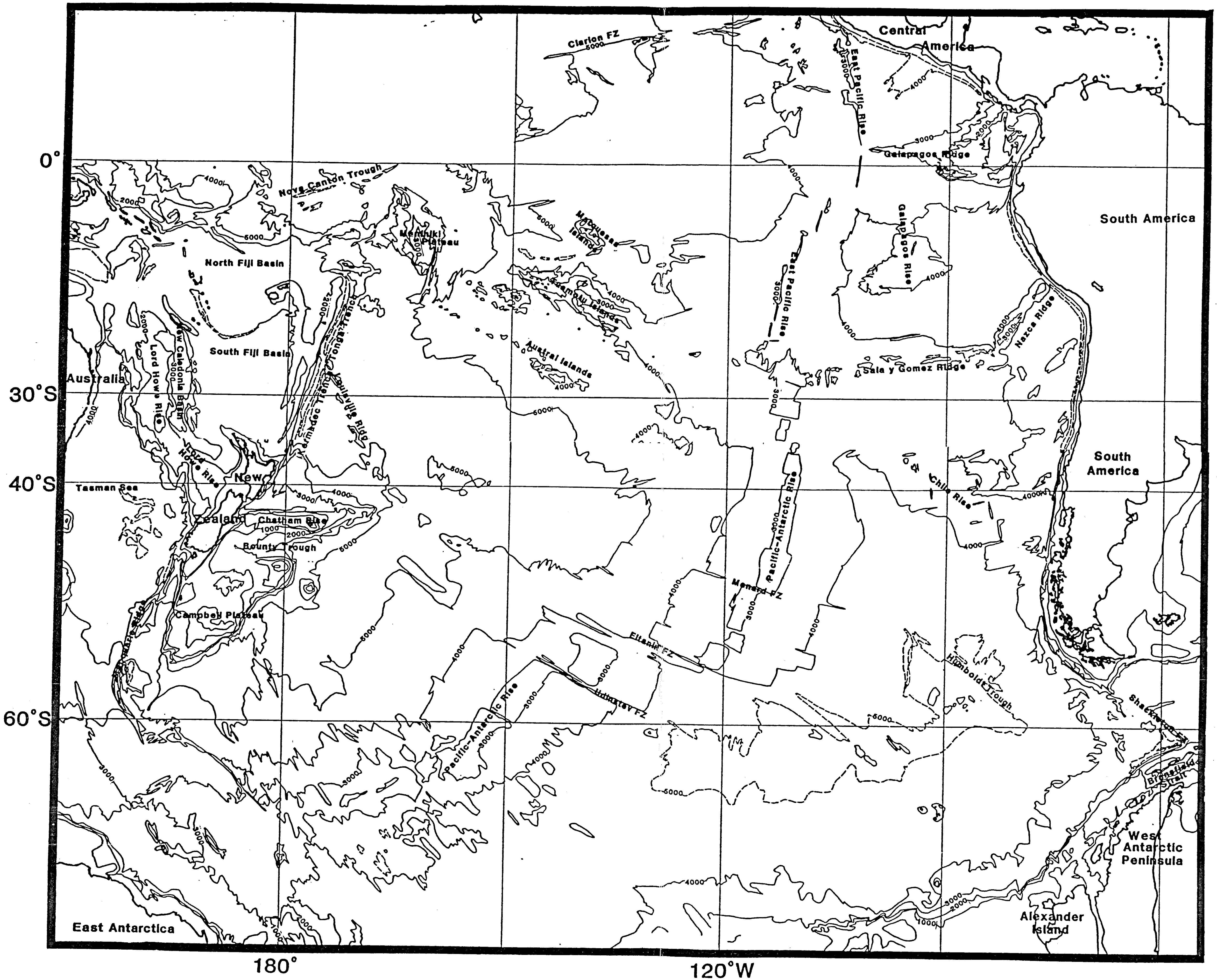

Central America
South America
South America
Australia
New Zealand
Tasman Sea
East Antarctica
West Antarctic Peninsula
Alexander Island
Clarion FZ
East Pacific Rise
Galapagos Ridge
Galapagos Rise
Nova Canton Trough
Manihiki Plateau
Marquesas Islands
Tuamotu Islands
Austral Islands
North Fiji Basin
South Fiji Basin
Lord Howe Rise
New Caledonia Basin
Kermadec Trench
Tonga Trench
Louisville Ridge
Nazca Ridge
Sala y Gomez Ridge
Chile Rise
Pacific-Antarctic Rise
Menard FZ
Eltanin FZ
Udintsev FZ
Humboldt Trough
Shackleton FZ
Bransfield Strait
Chatham Rise
Bounty Trough
Campbell Plateau
0°
30°S
40°S
60°S
180°
120°W

1a

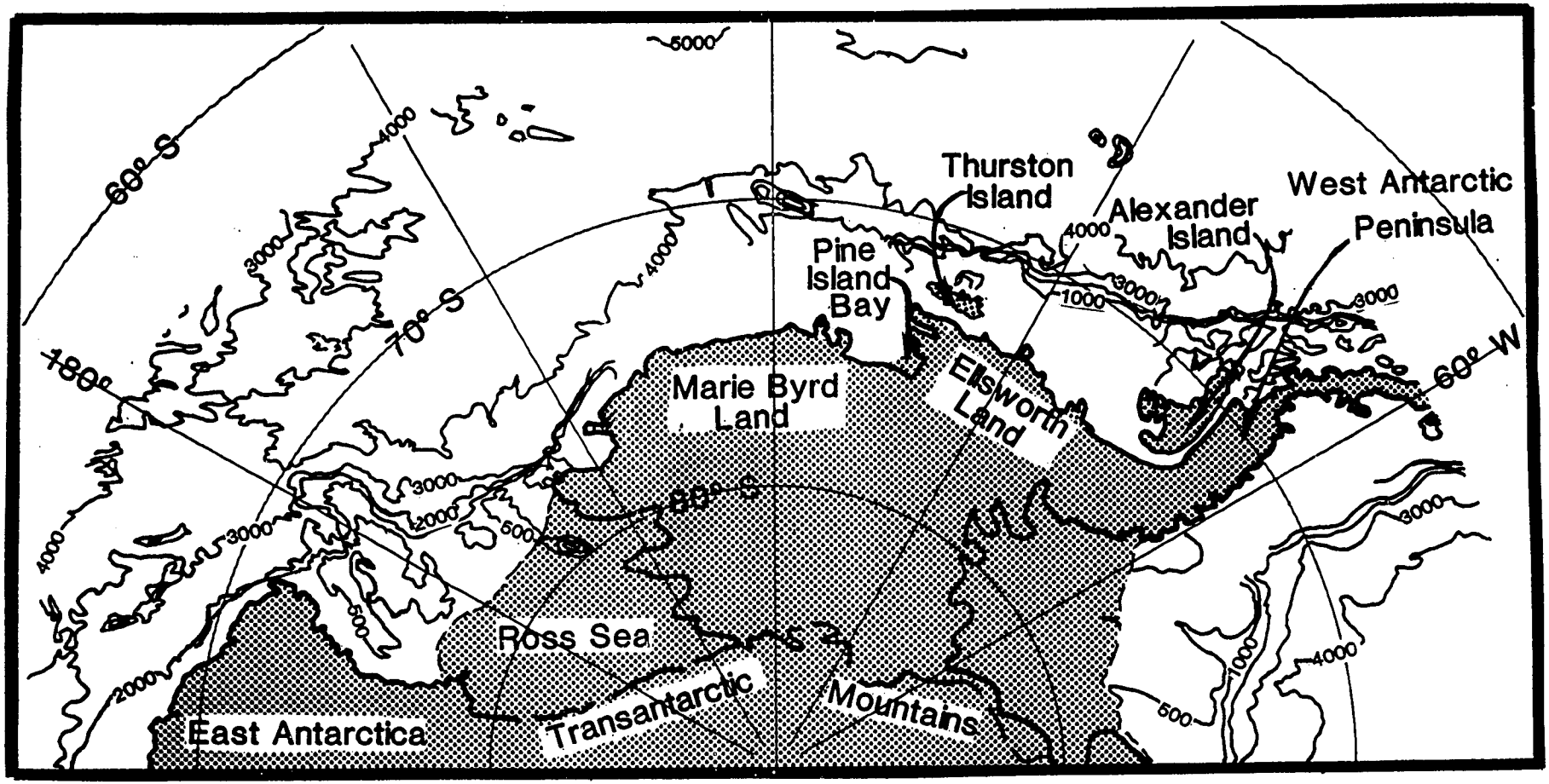
Thurston Island
Alexander Island
West Antarctic Peninsula
Pine Island Bay
Marie Byrd Land
Ellsworth Land
Ross Sea
Transantarctic Mountains
East Antarctica
60° S
70° S
80° S
180°
60° W
5000
4000
3000
2000
1000
600
500

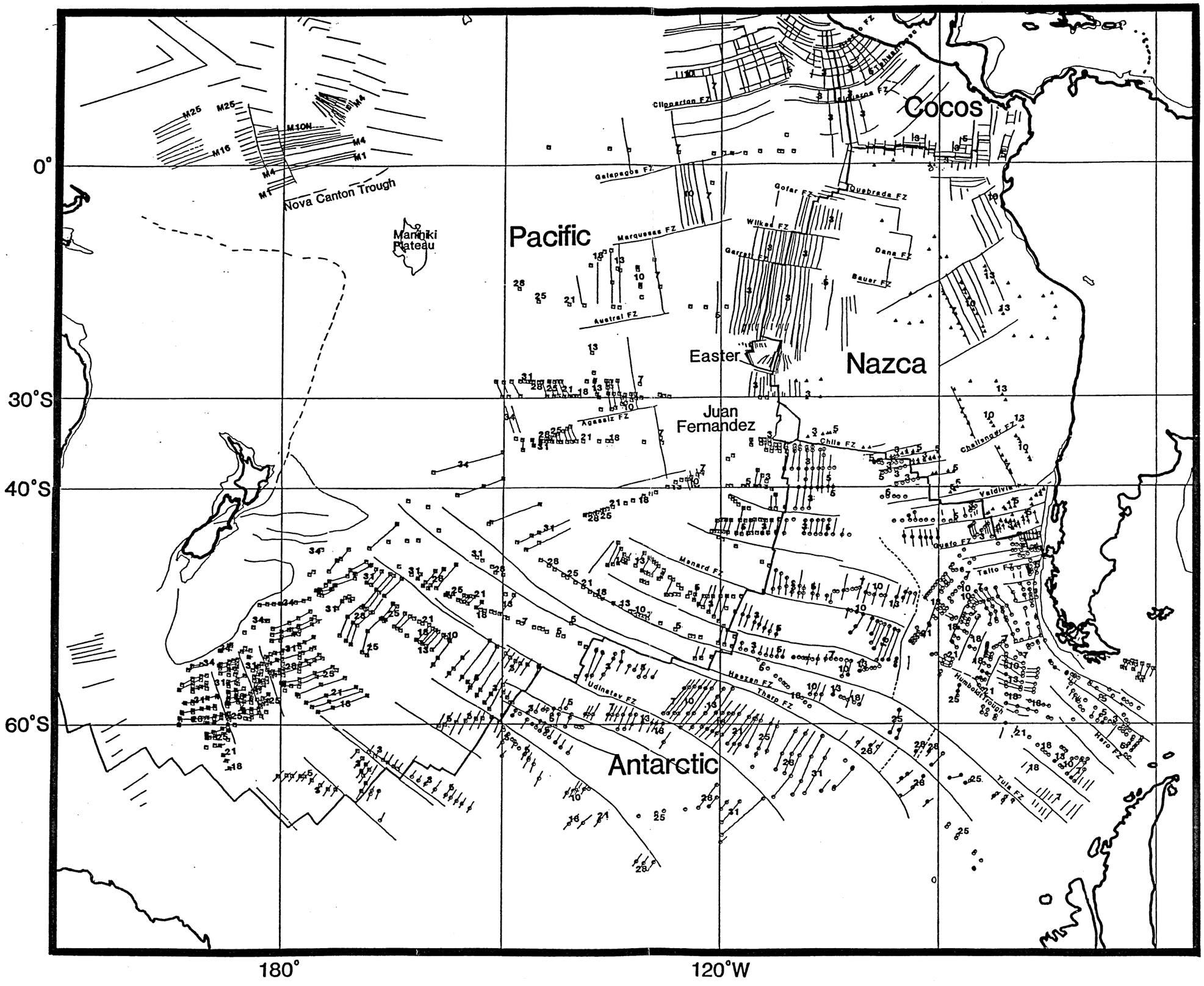
Cocos
Pacific
Nazca
Easter
Juan Fernandez
Antarctic
Nova Canton Trough
Manihiki Plateau
Galapagos FZ
Clipperton FZ
Marquesas FZ
Austral FZ
Gofar FZ
Quebrada FZ
Wilkes FZ
Garrett FZ
Dana FZ
Bauer FZ
Agassiz FZ
Chile FZ
Challenger FZ
Valdivia
Guafo FZ
Taito FZ
Menard FZ
Udintsev FZ
Heezen FZ
Thero FZ
Humboldt Trough
Tula FZ
Hero FZ
M25
M16
M10N
M4
M1
0°
30°S
40°S
60°S
180°
120°W

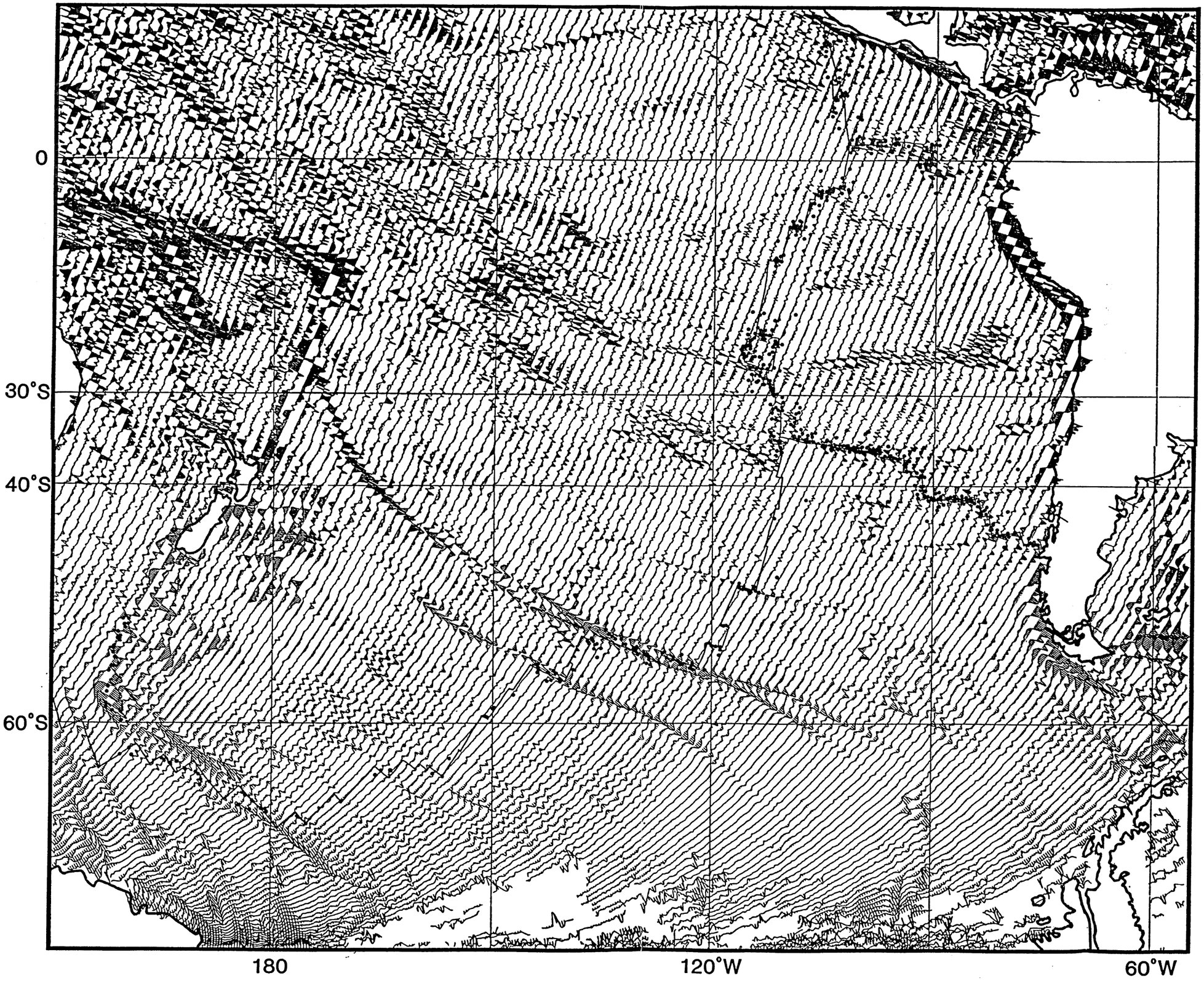
0
30°S
40°S
60°S
180
120°W
60°W

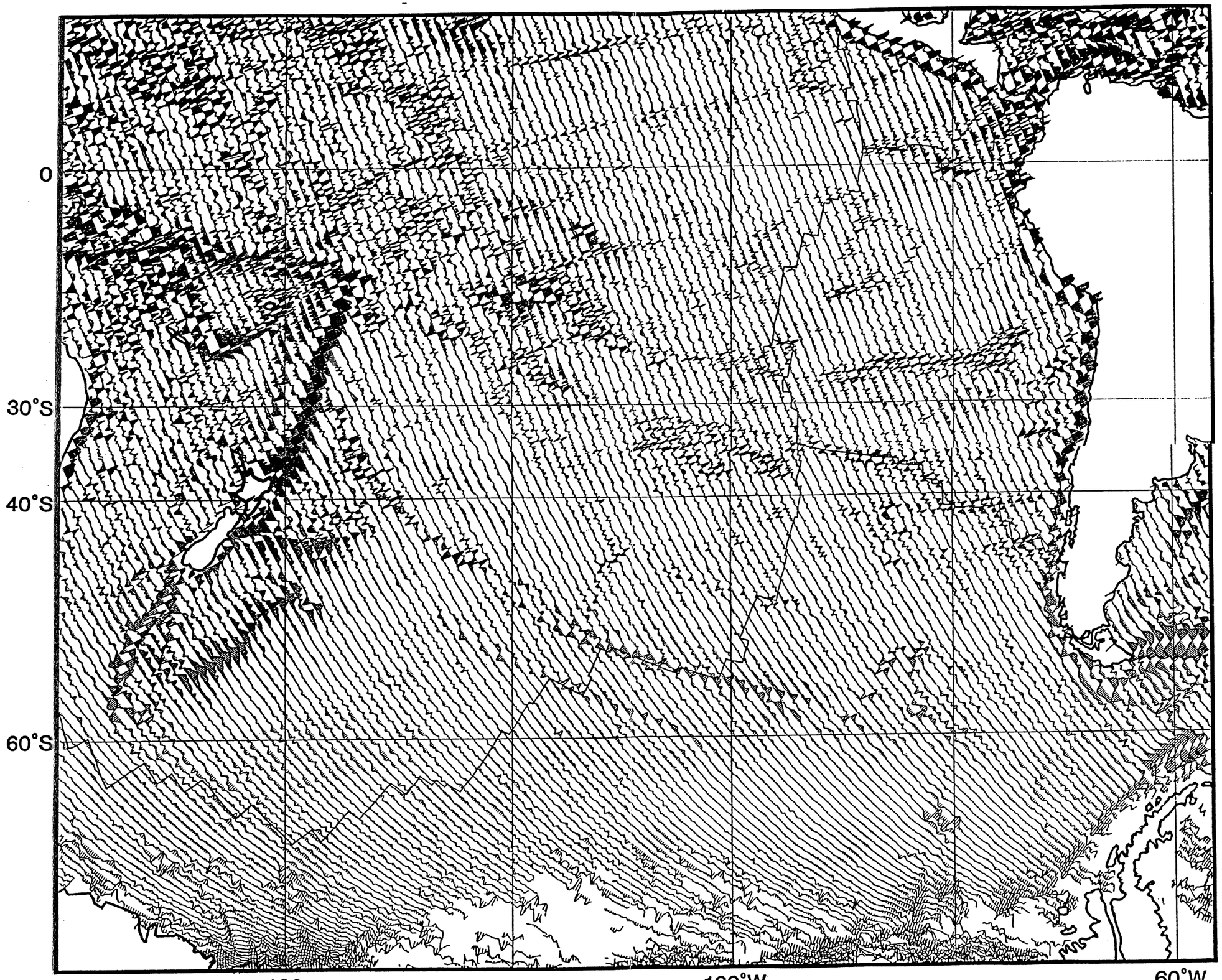
0
30°S
40°S
60°S
180
120°W
60°W

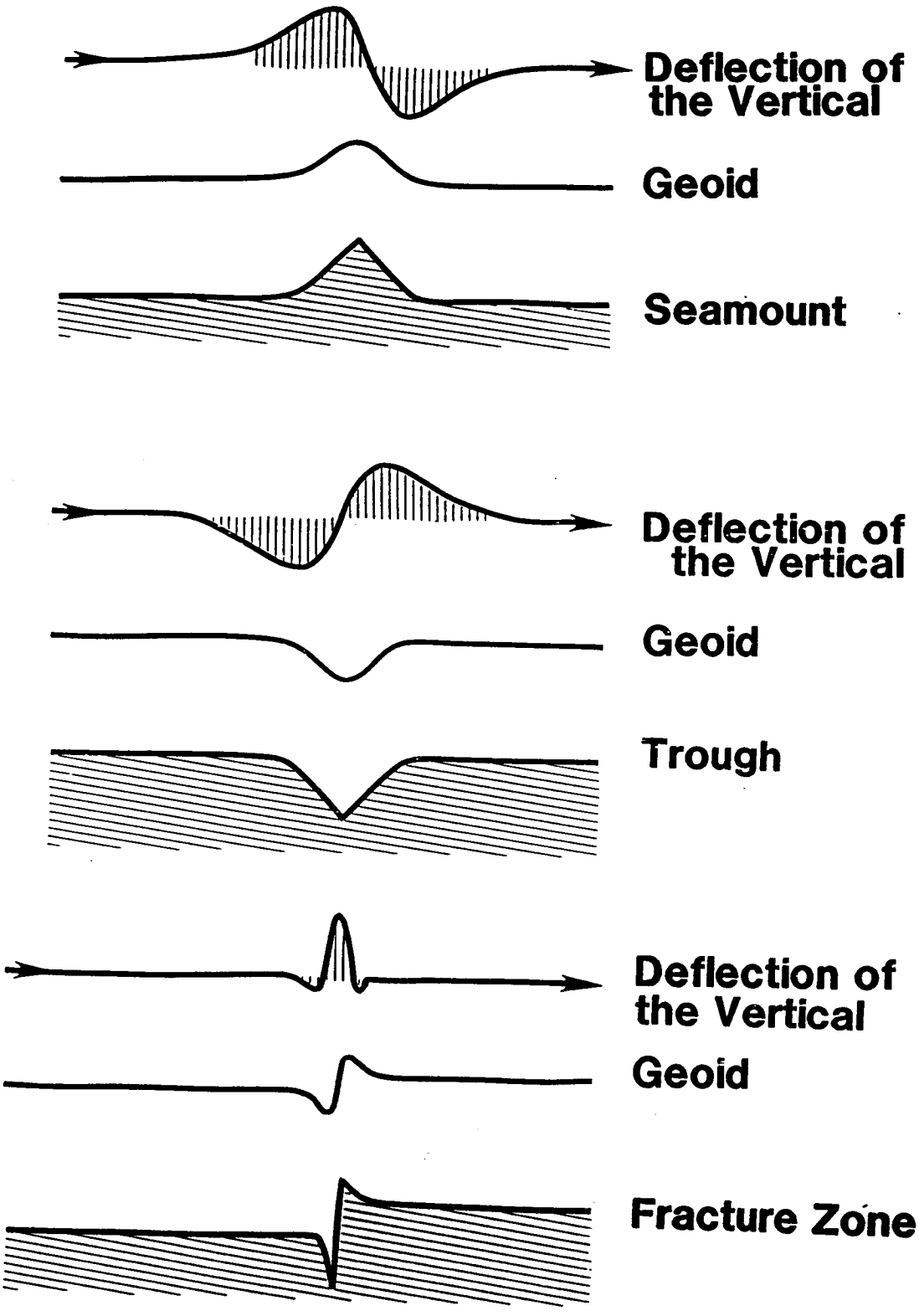
Deflection of the Vertical
Geoid
Seamount
Deflection of the Vertical
Geoid
Trough
Deflection of the Vertical
Geoid
Fracture Zone

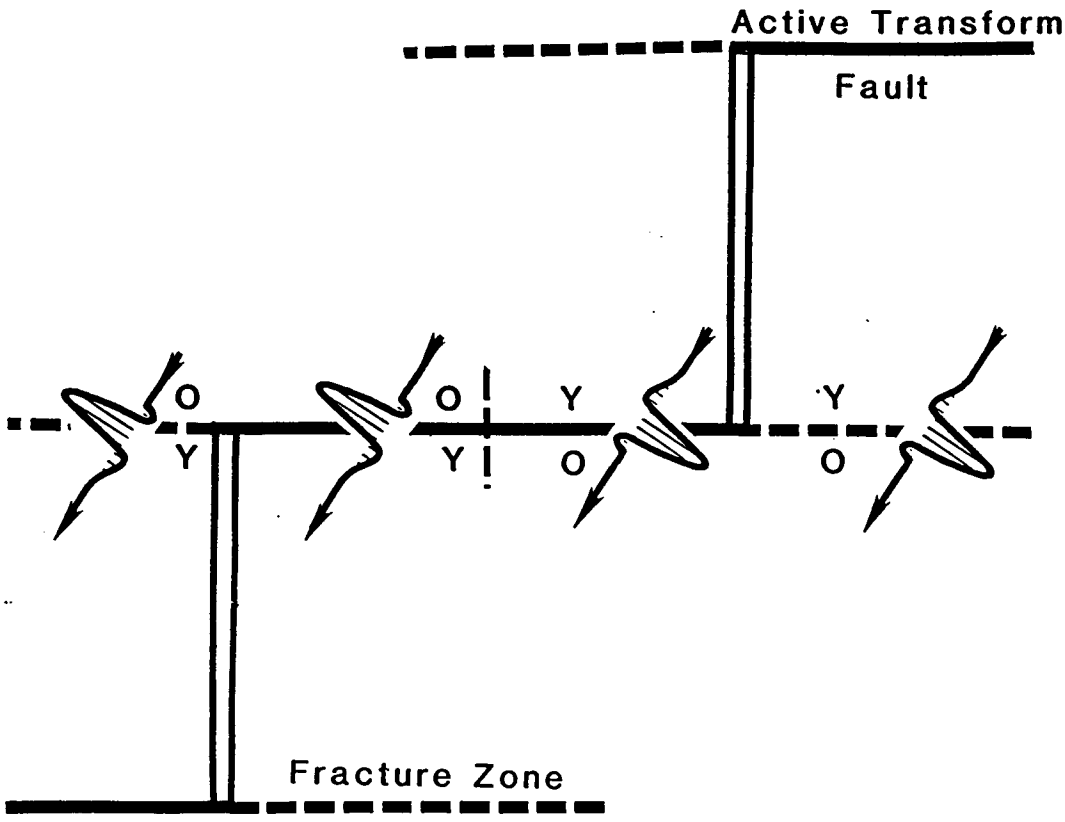
Active Transform
Fault
O
Y
O
Y
Y
O
Y
O
Fracture Zone

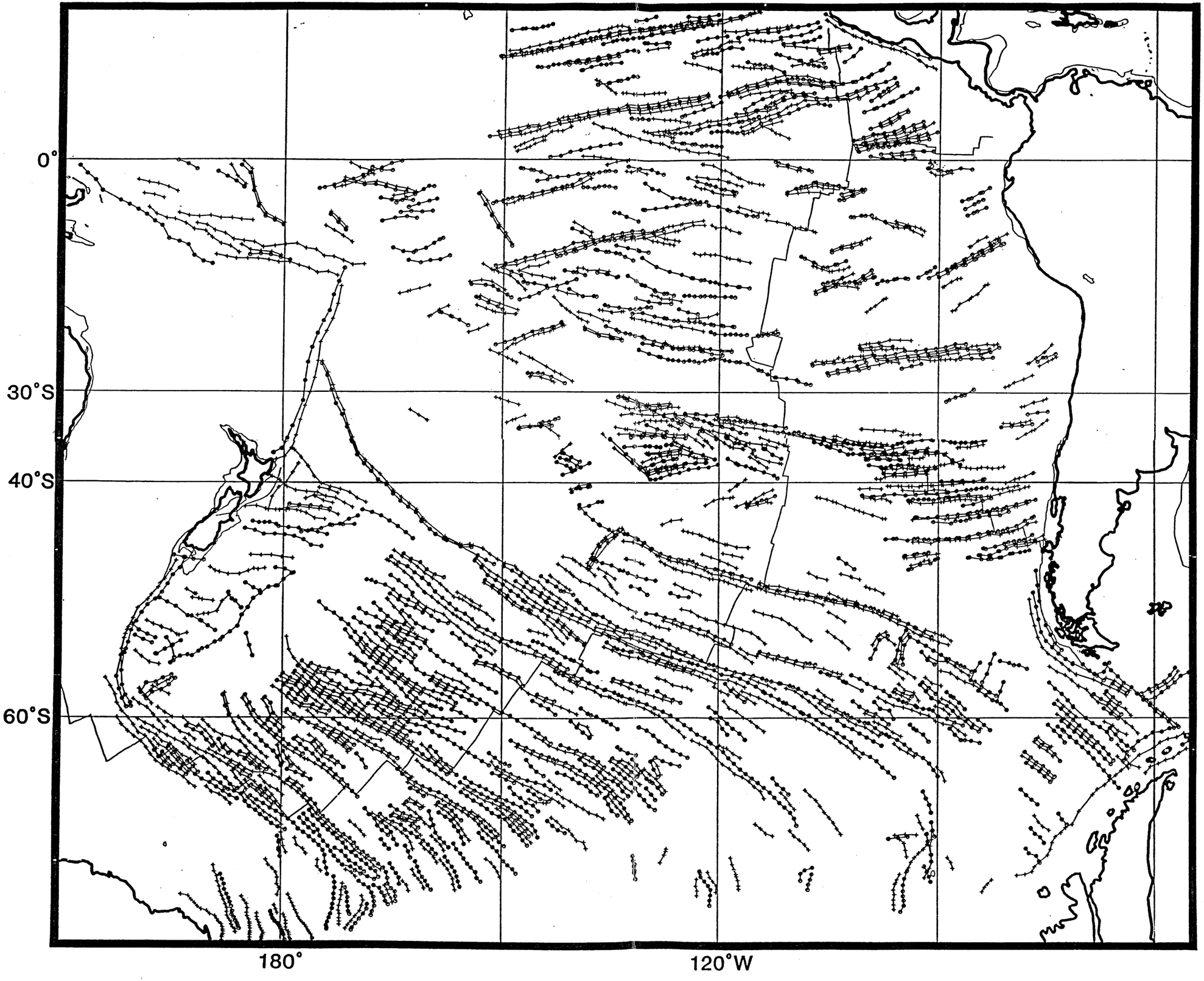
0°
30°S
40°S
60°S
180°
120°W

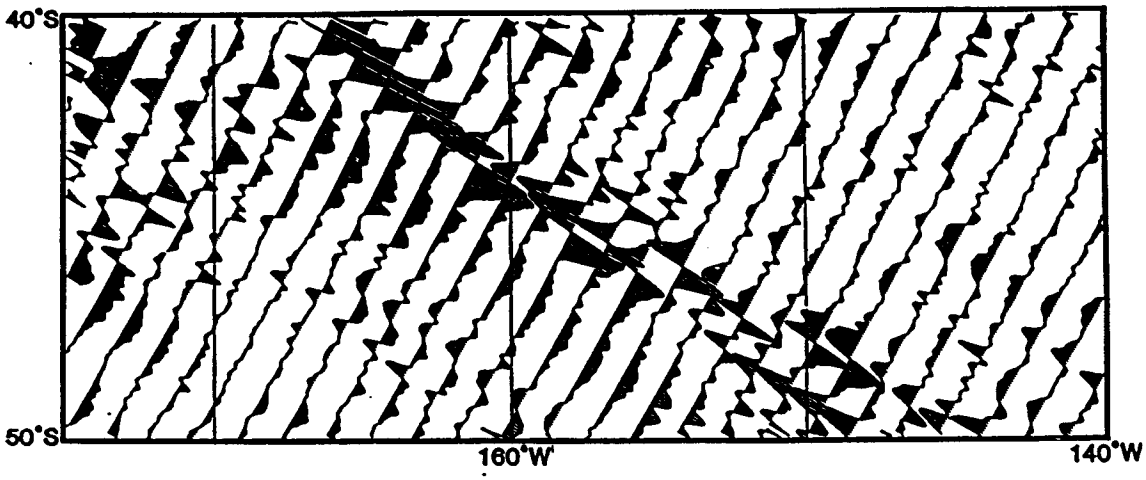
40°S
50°S
160°W
140°W

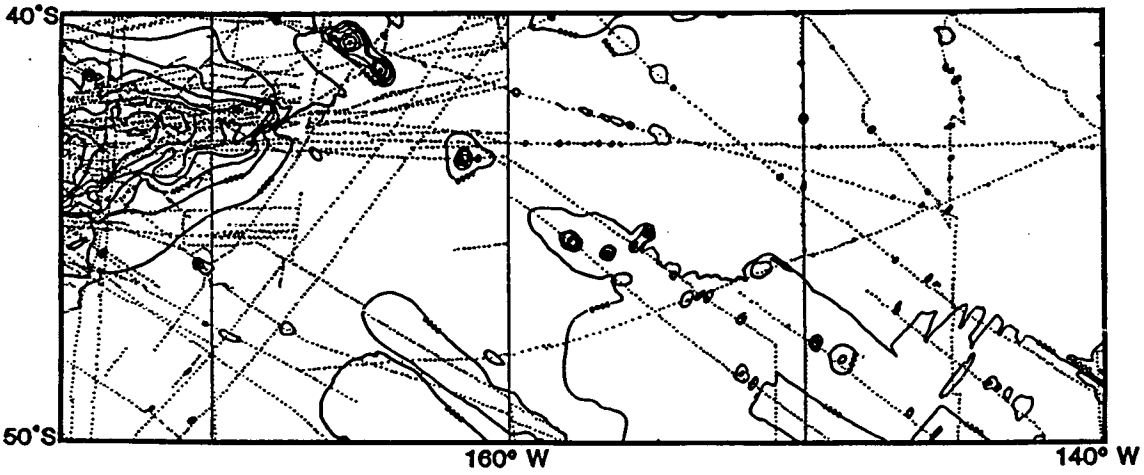
40°S
50°S
160° W
140° W

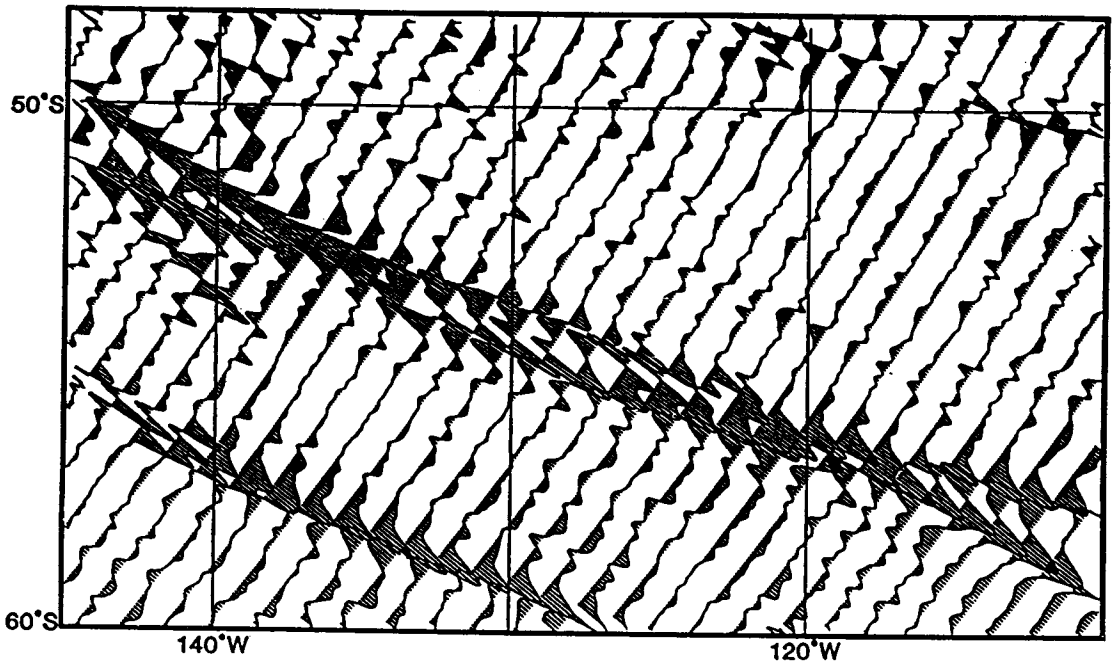
50°S
60°S
140°W
120°W

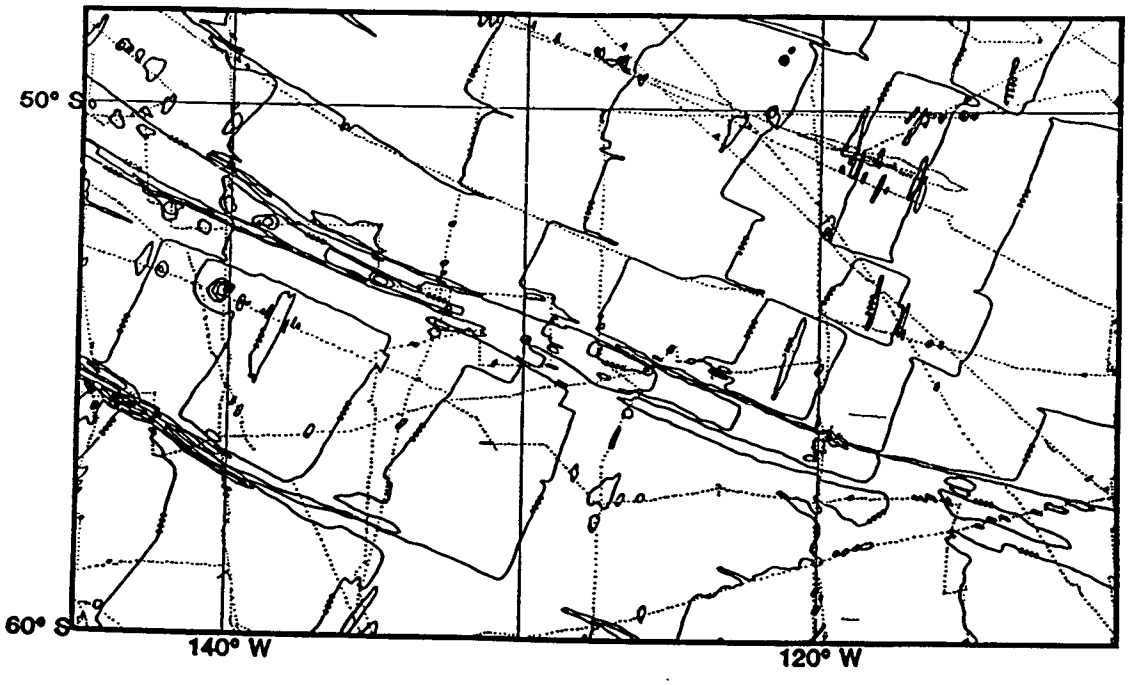
50° S
60° S
140° W
120° W

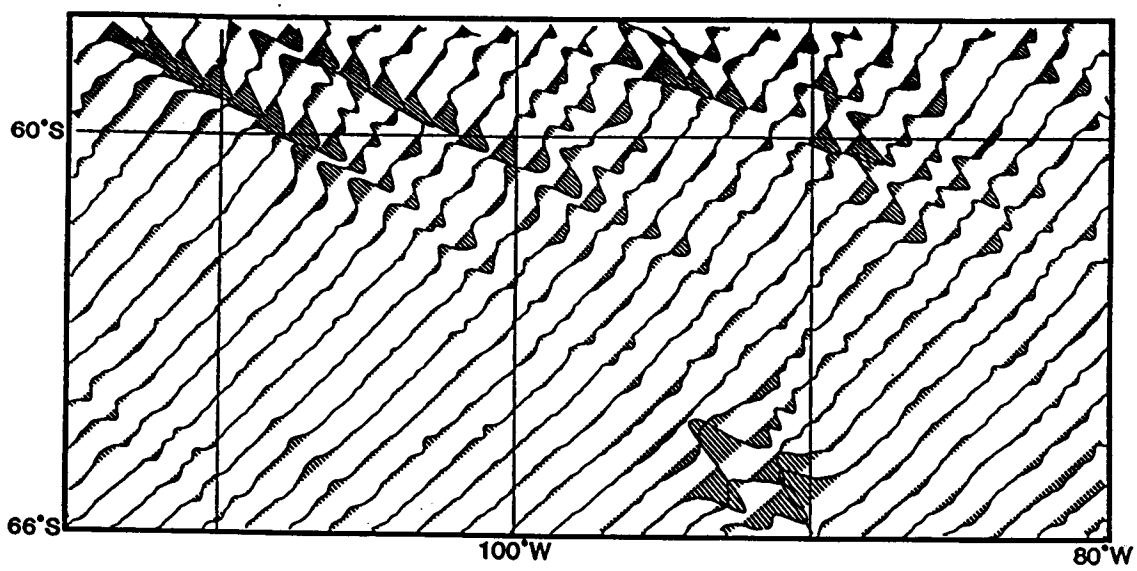

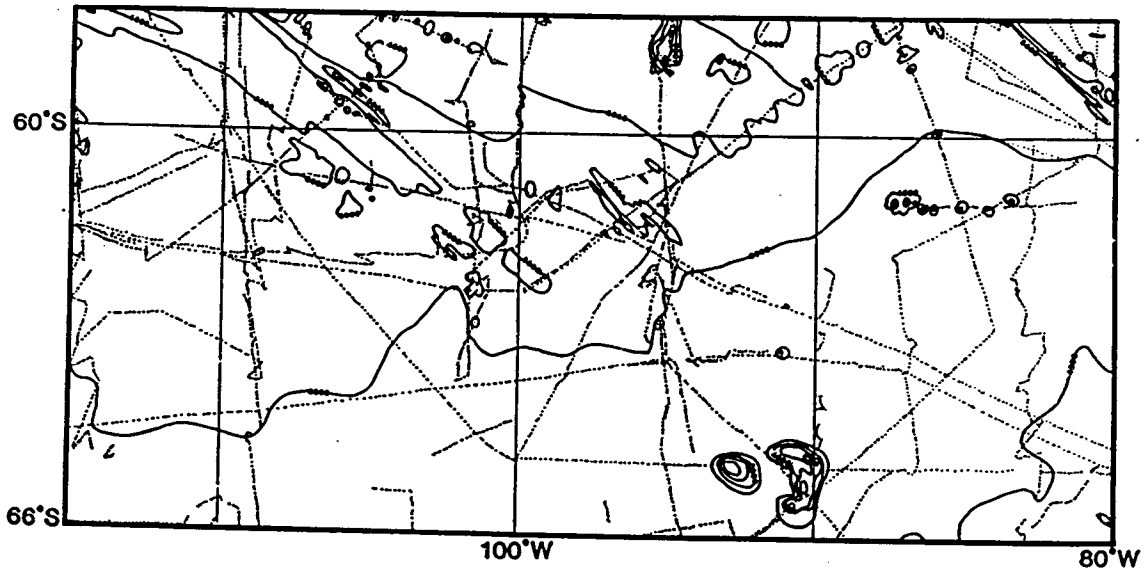

6c

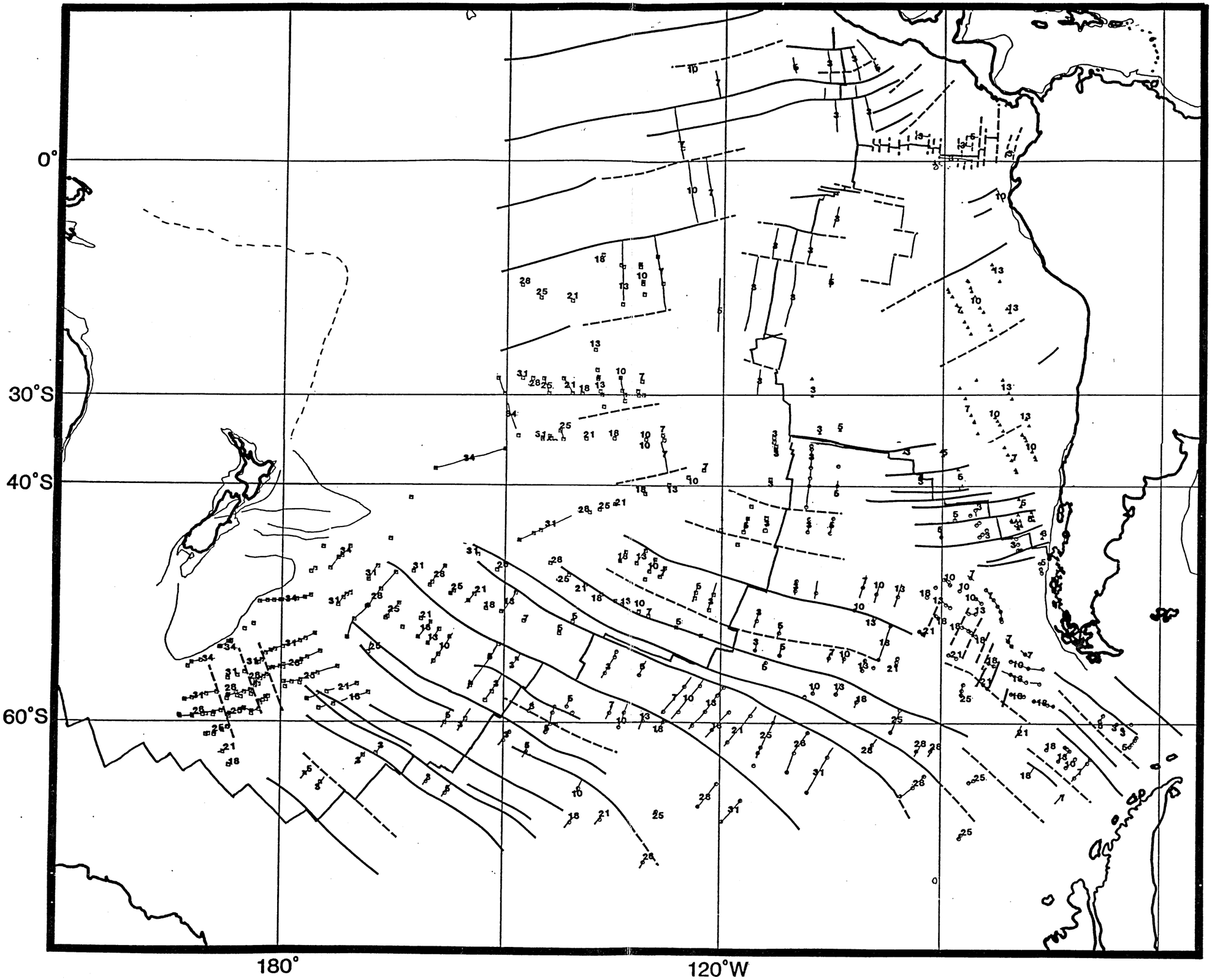
0°
30°S
40°S
60°S
180°
120°W

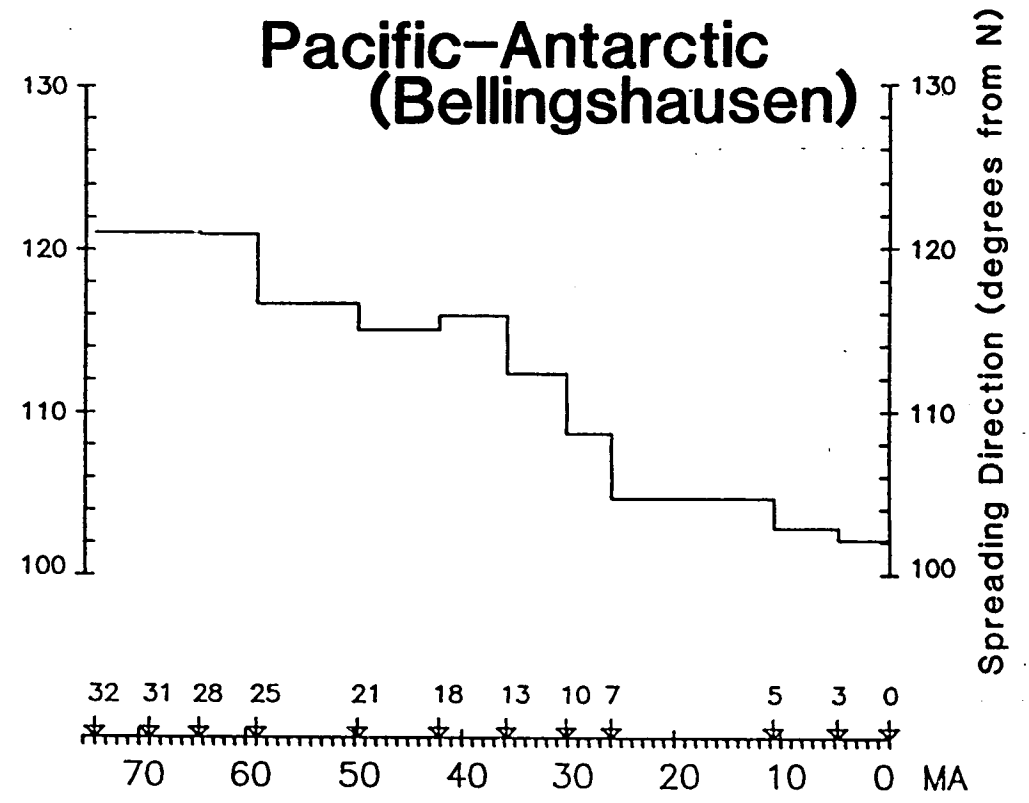
Pacific–Antarctic
(Bellingshausen)
130
120
110
100
Spreading Direction (degrees from N)
32 31 28 25 21 18 13 10 7 5 3 0
70 60 50 40 30 20 10 0 MA

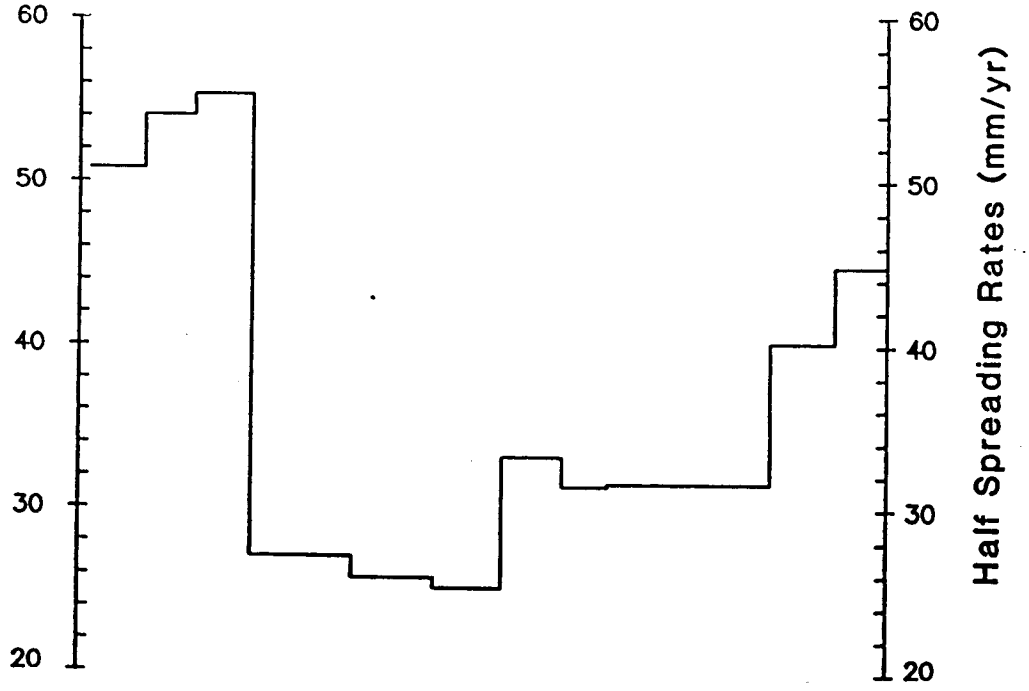
60
50
40
30
20
Half Spreading Rates (mm/yr)

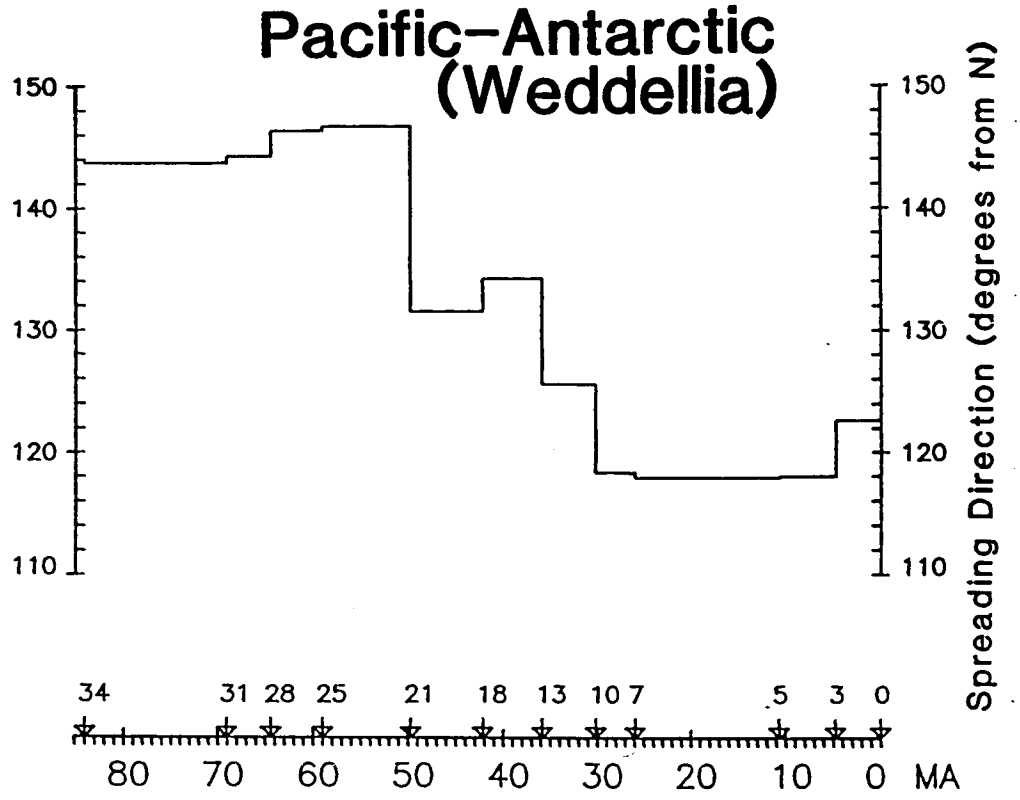
Pacific–Antarctic
(Weddellia)
150
140
130
120
110
Spreading Direction (degrees from N)
34
31
28
25
21
18
13
10
7
5
3
0
80
70
60
50
40
30
20
10
0
MA

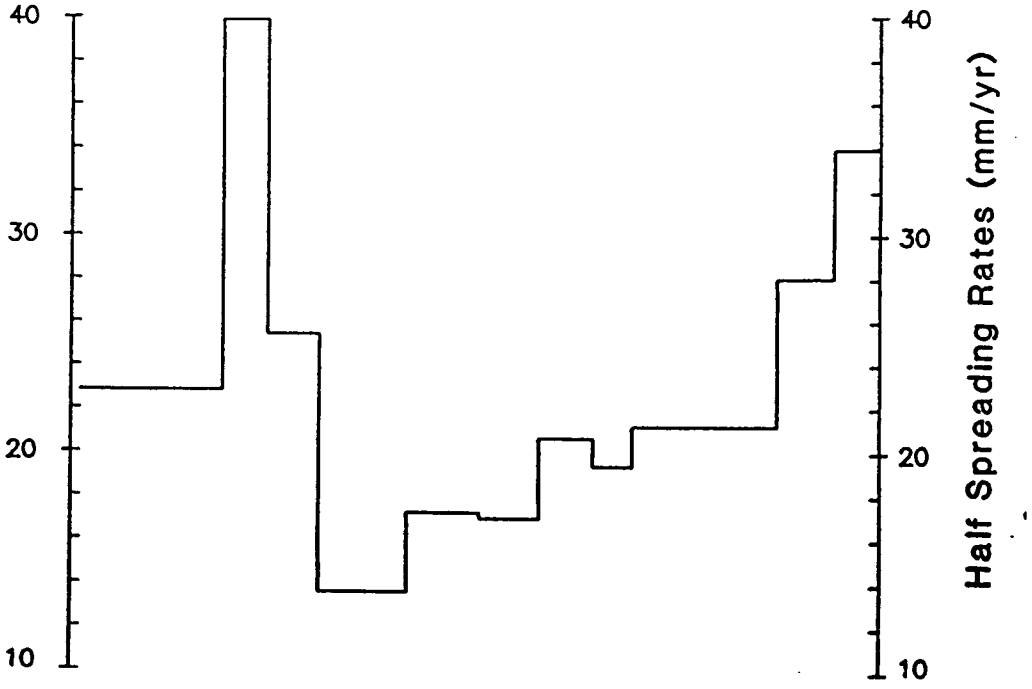
40
30
20
10
Half Spreading Rates (mm/yr)

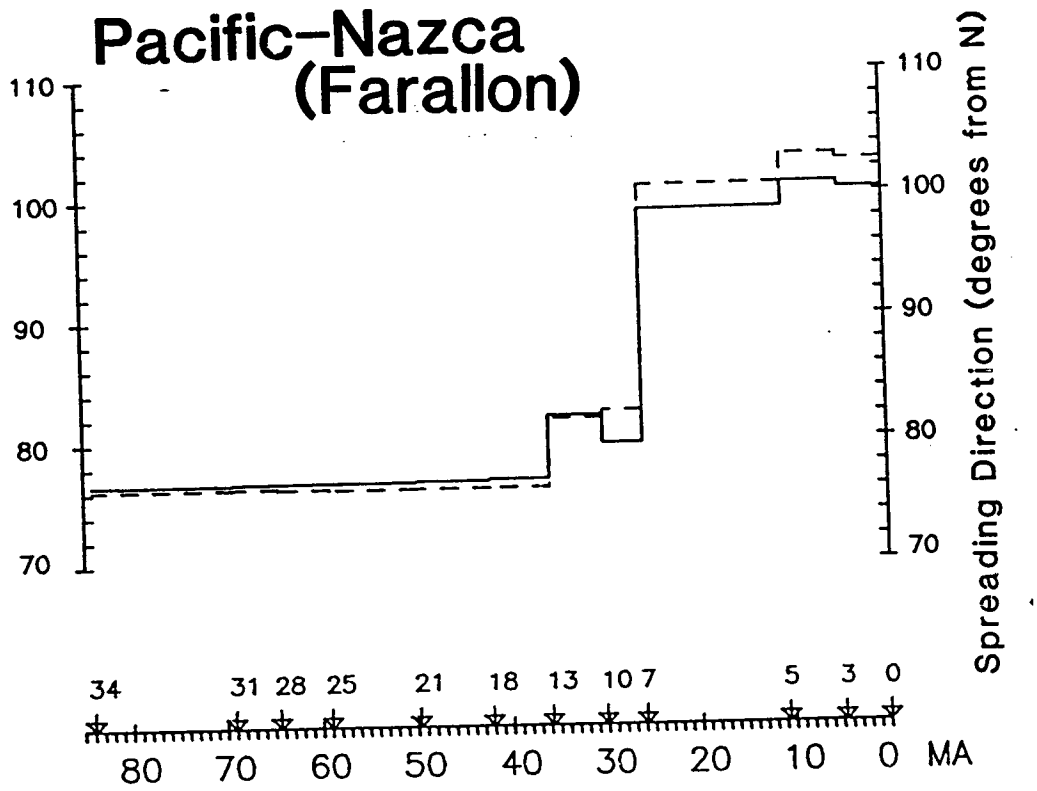
Pacific–Nazca
(Farallon)
110
100
90
80
70
Spreading Direction (degrees from N)
34
31
28
25
21
18
13
10
7
5
3
0
80
70
60
50
40
30
20
10
0
MA

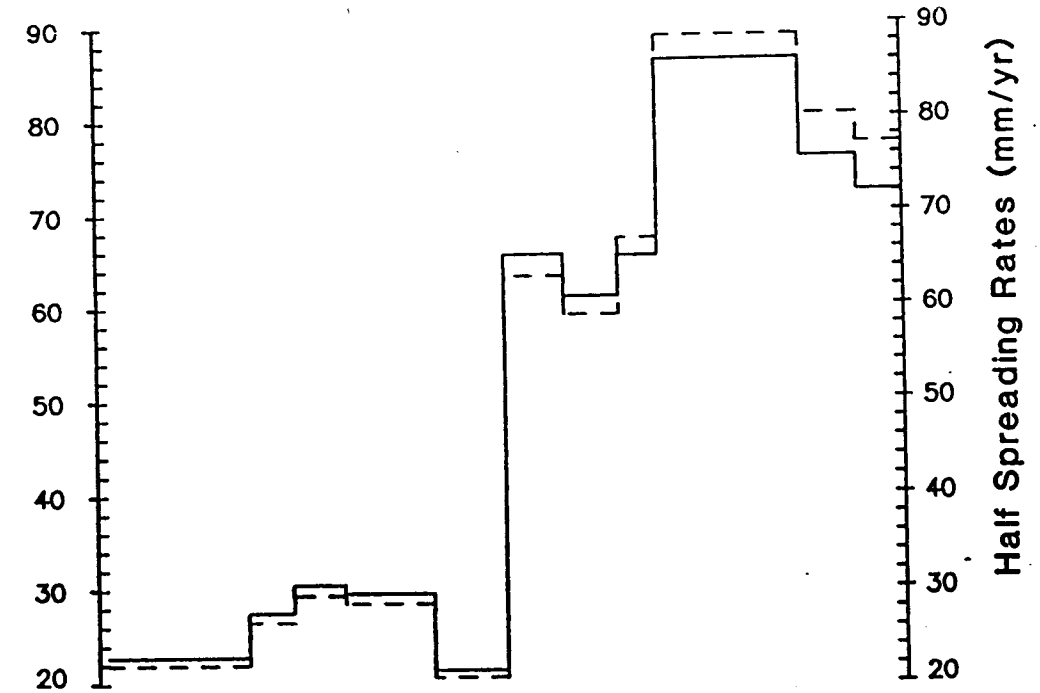
90
80
70
60
50
40
30
20
Half Spreading Rates (mm/yr)

8C

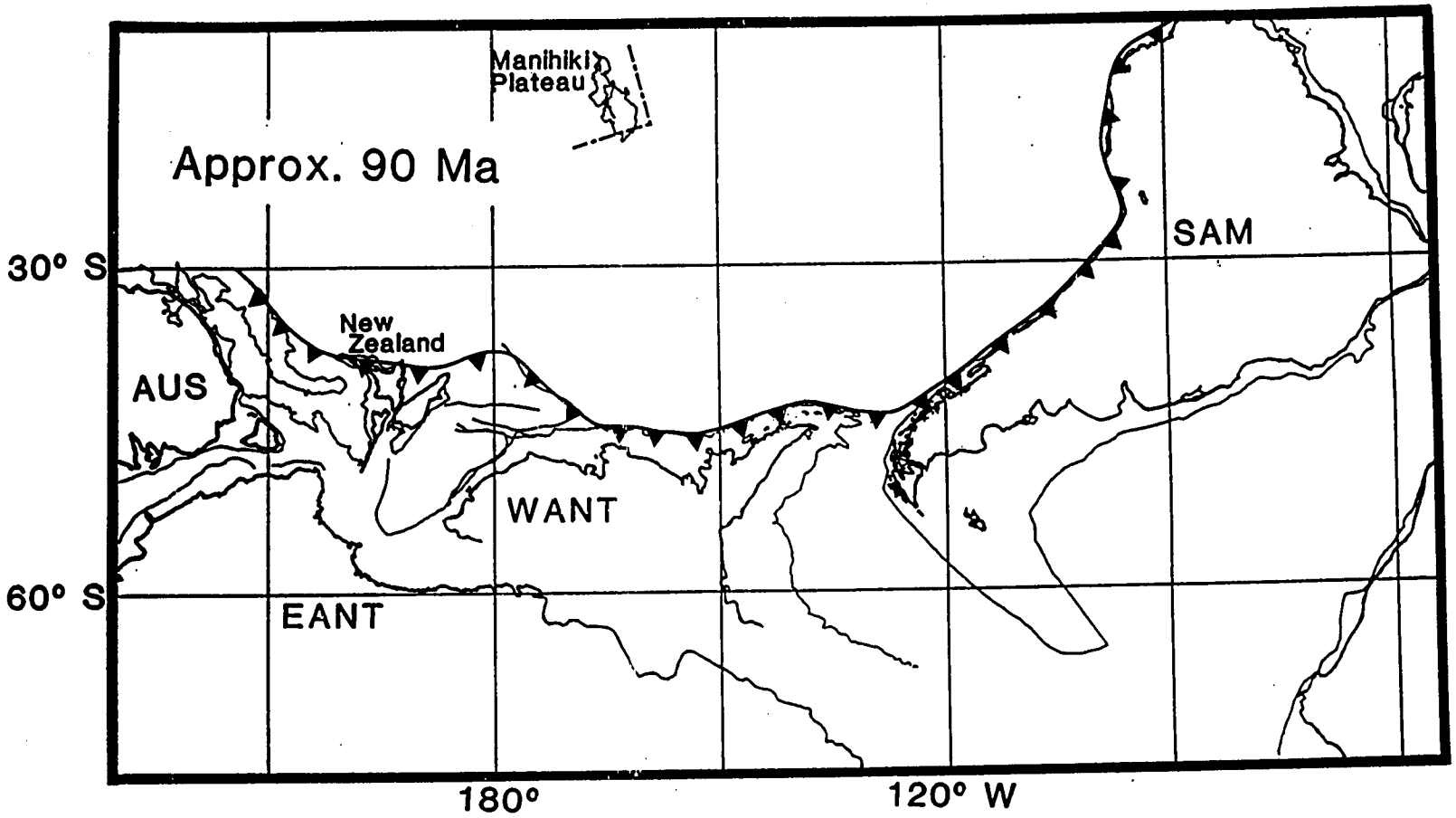
Manihiki Plateau
Approx. 90 Ma
30° S
60° S
New Zealand
AUS
SAM
WANT
EANT
180°
120° W

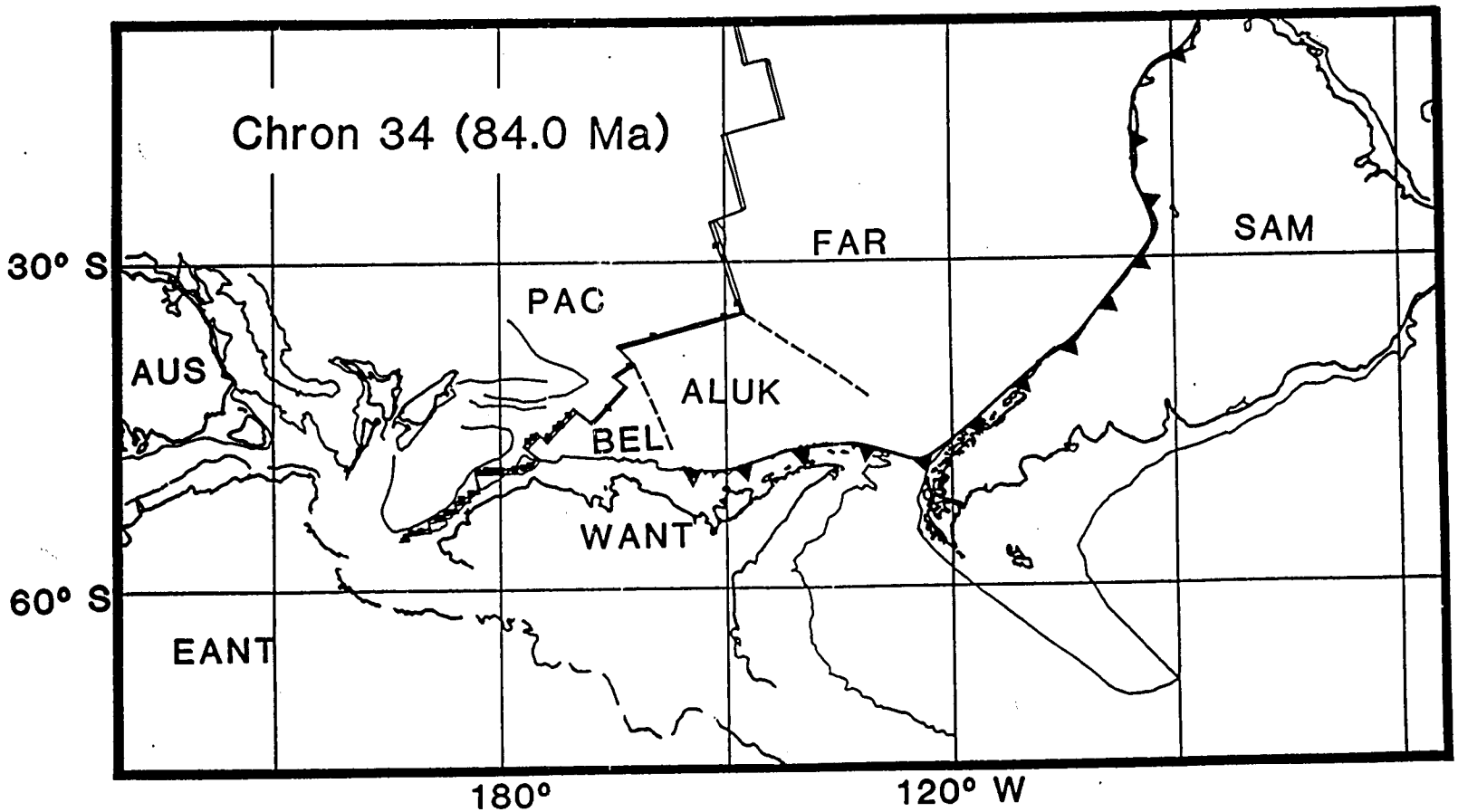
Chron 34 (84.0 Ma)
30° S
60° S
180°
120° W
FAR
SAM
PAC
AUS
ALUK
BEL
WANT
EANT

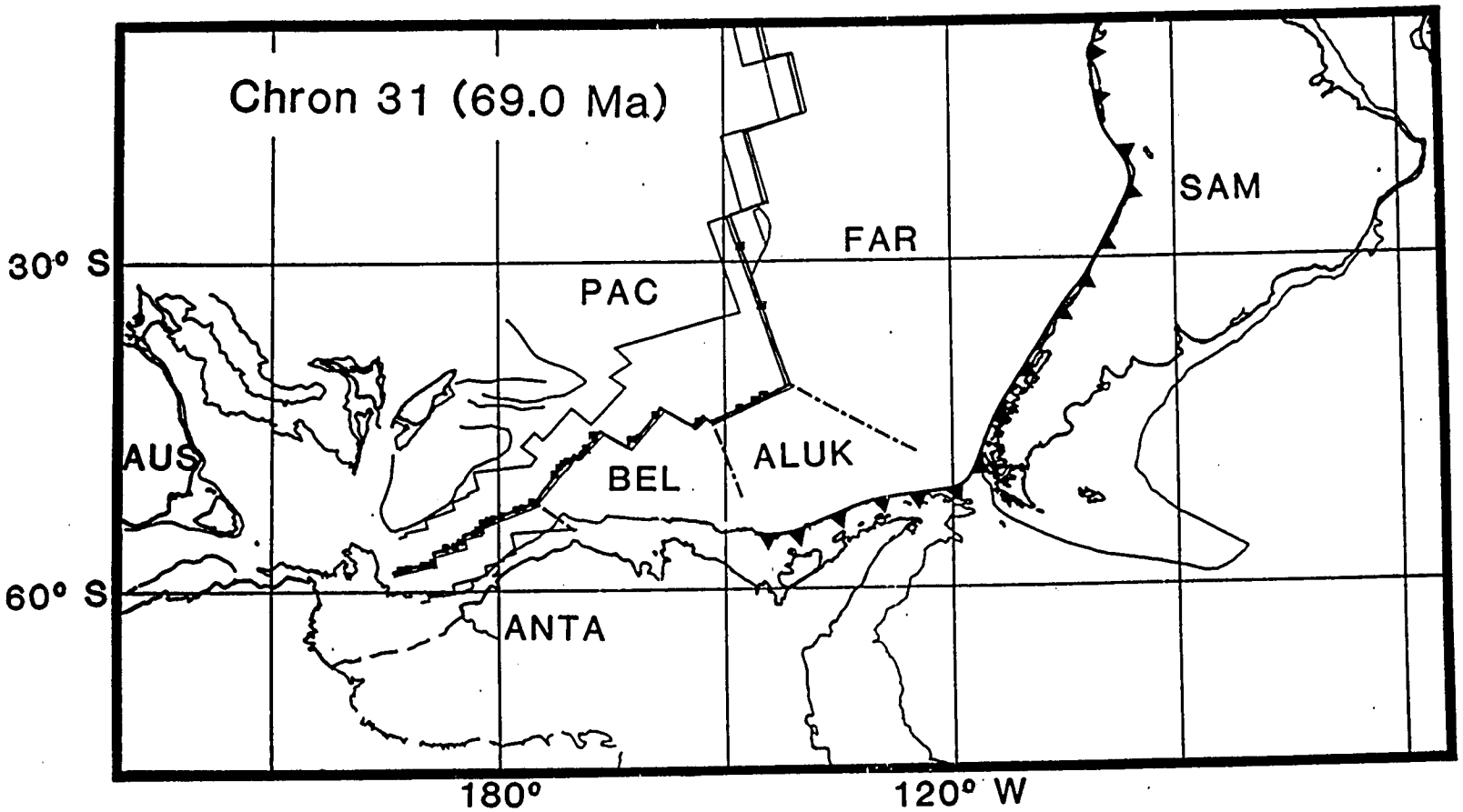
Chron 31 (69.0 Ma)
30° S
60° S
180°
120° W
SAM
FAR
PAC
AUS
BEL
ALUK
ANTA

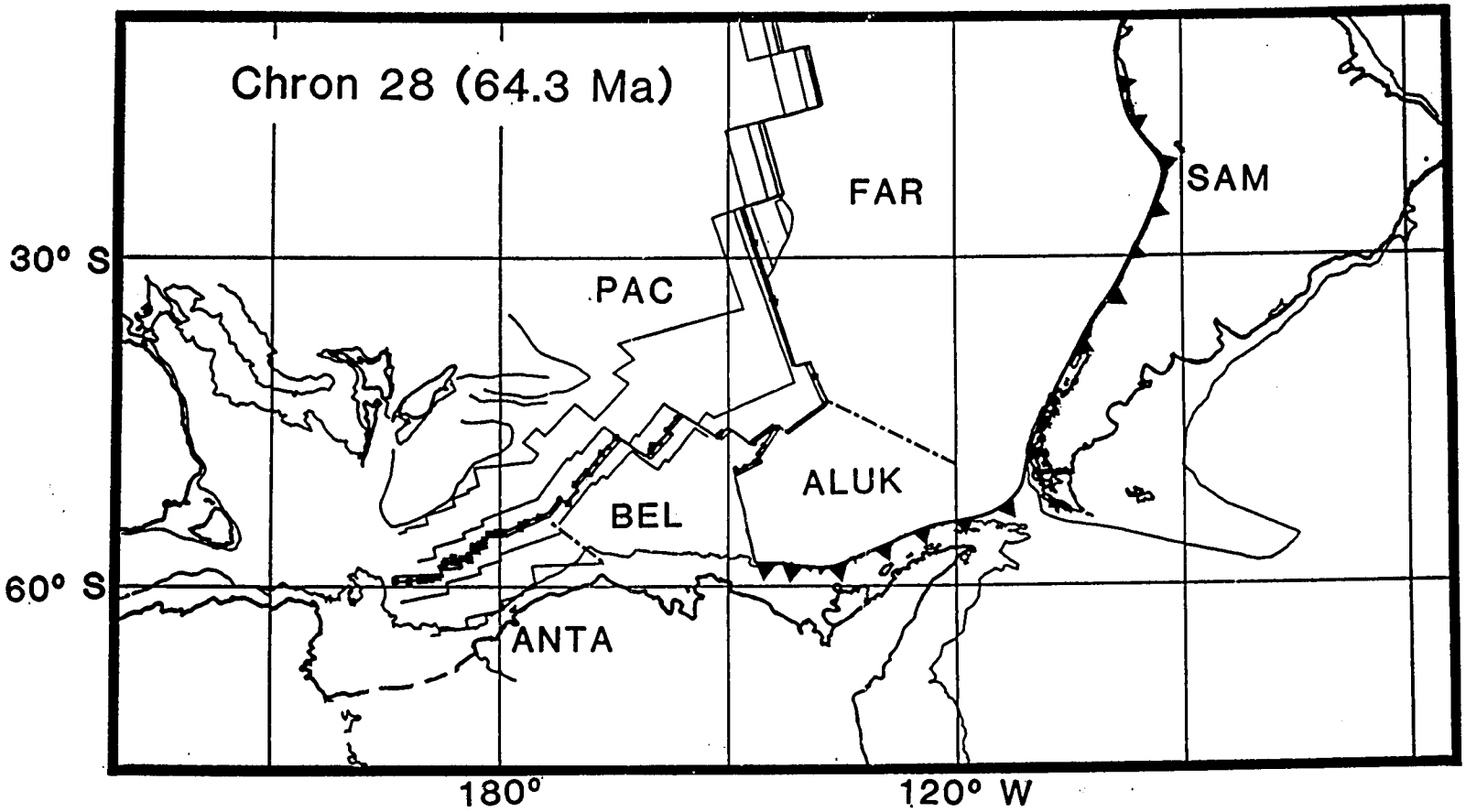
Chron 28 (64.3 Ma)
FAR
SAM
30° S
PAC
ALUK
BEL
60° S
ANTA
180°
120° W

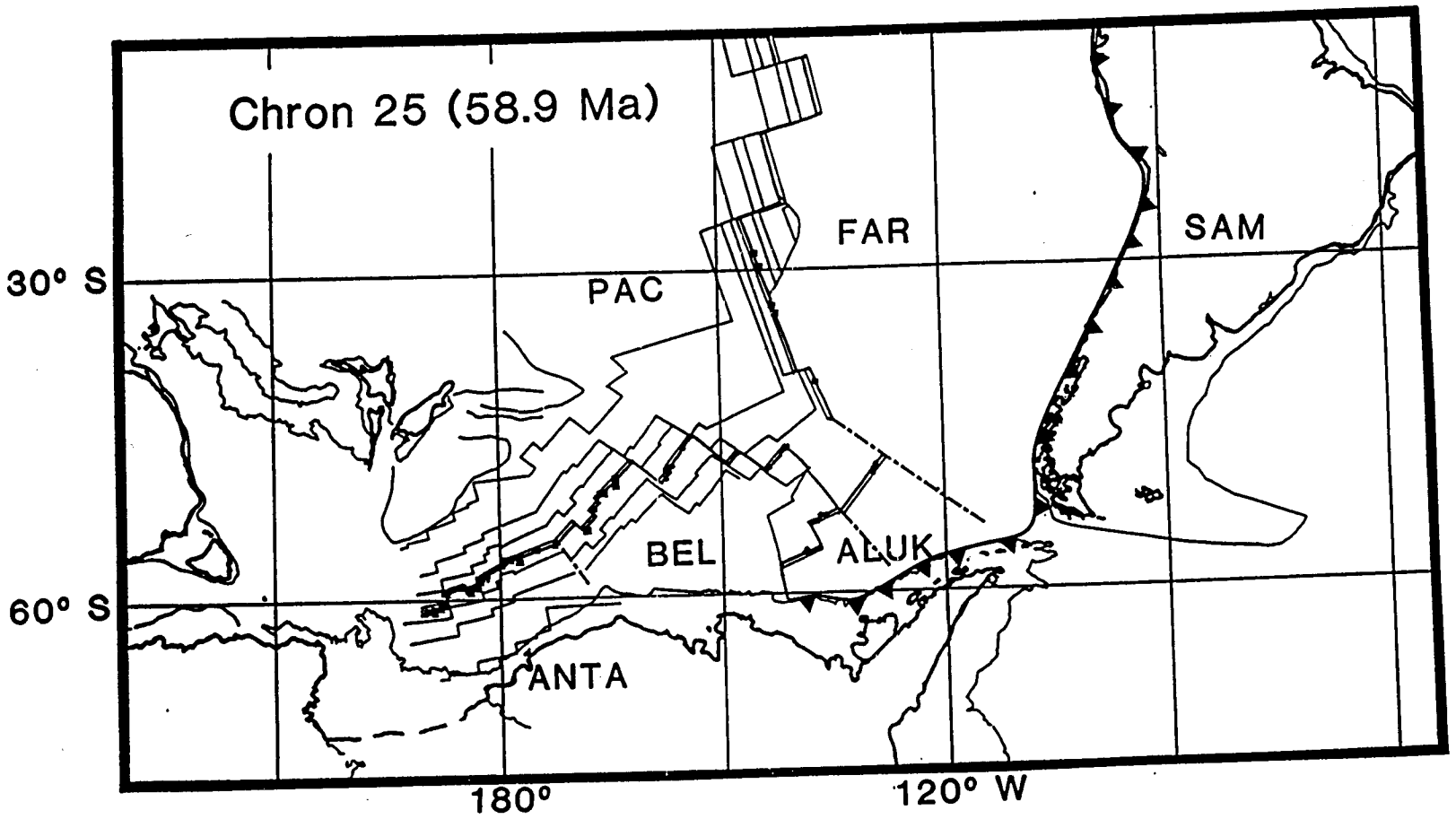
Chron 25 (58.9 Ma)
FAR
SAM
PAC
30° S
BEL
ALUK
60° S
ANTA
180°
120° W

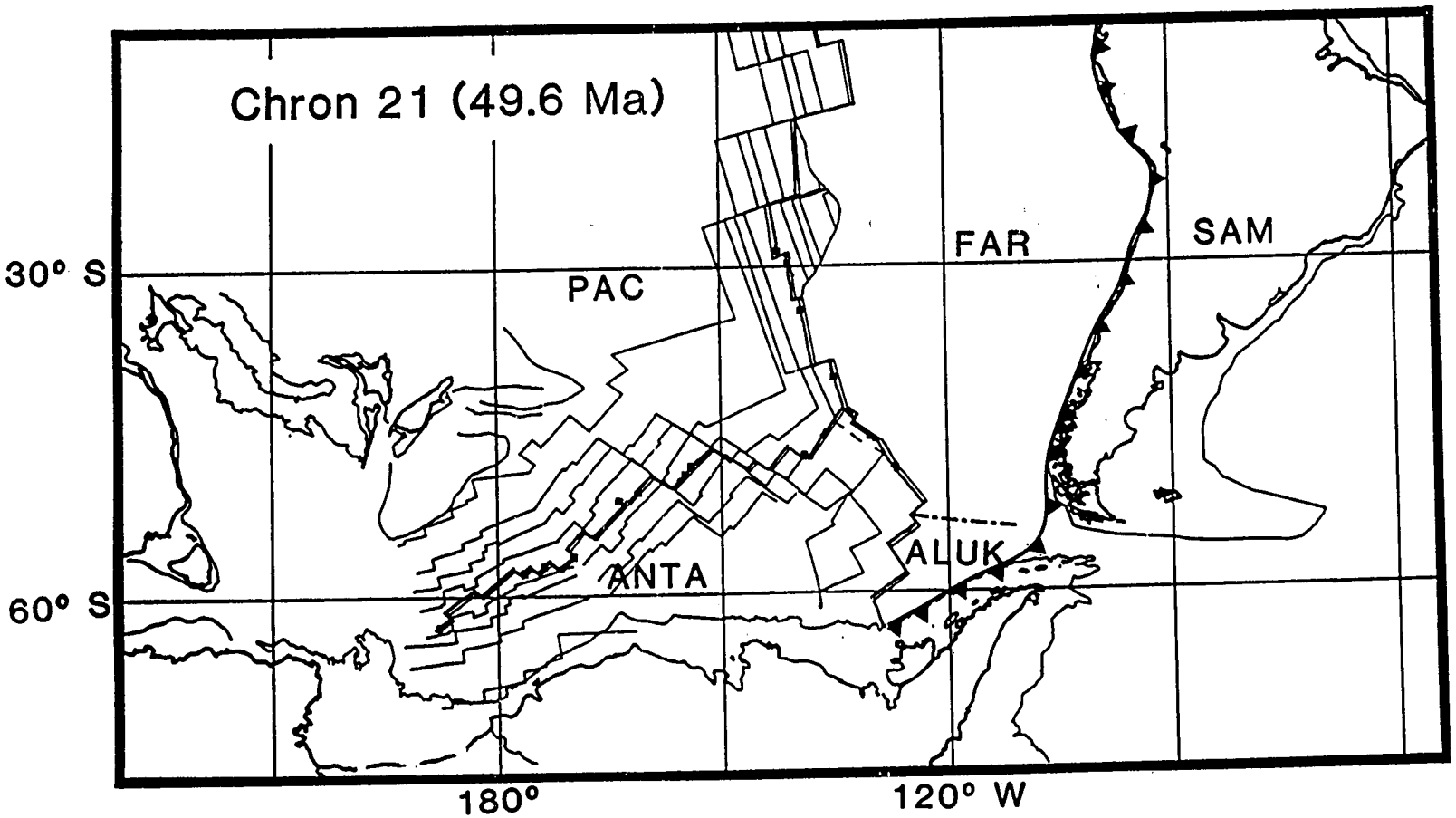
Chron 21 (49.6 Ma)
30° S
60° S
PAC
FAR
SAM
ANTA
ALUK
180°
120° W

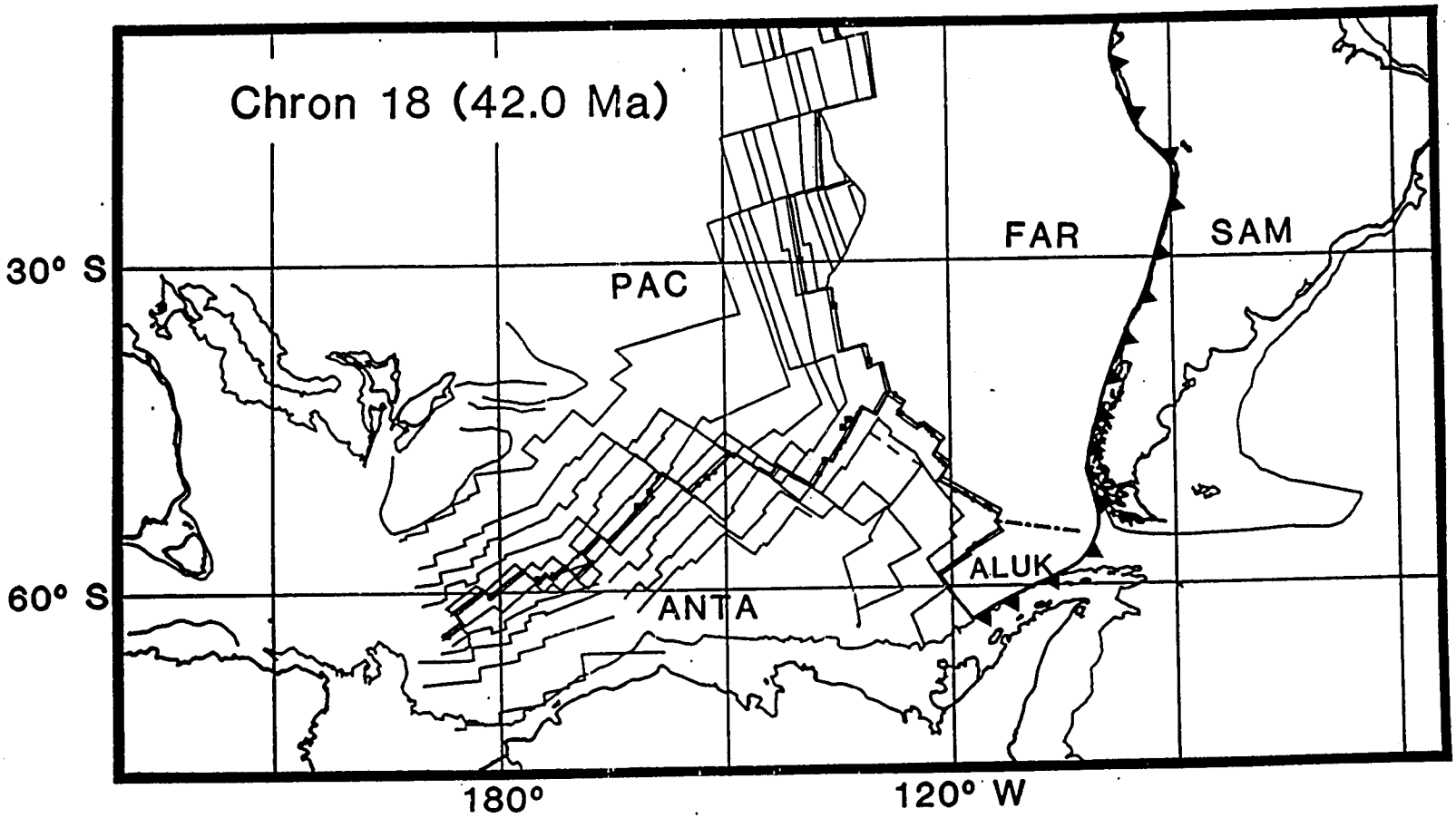
Chron 18 (42.0 Ma)
30° S
60° S
180°
120° W
PAC
FAR
SAM
ALUK
ANTA

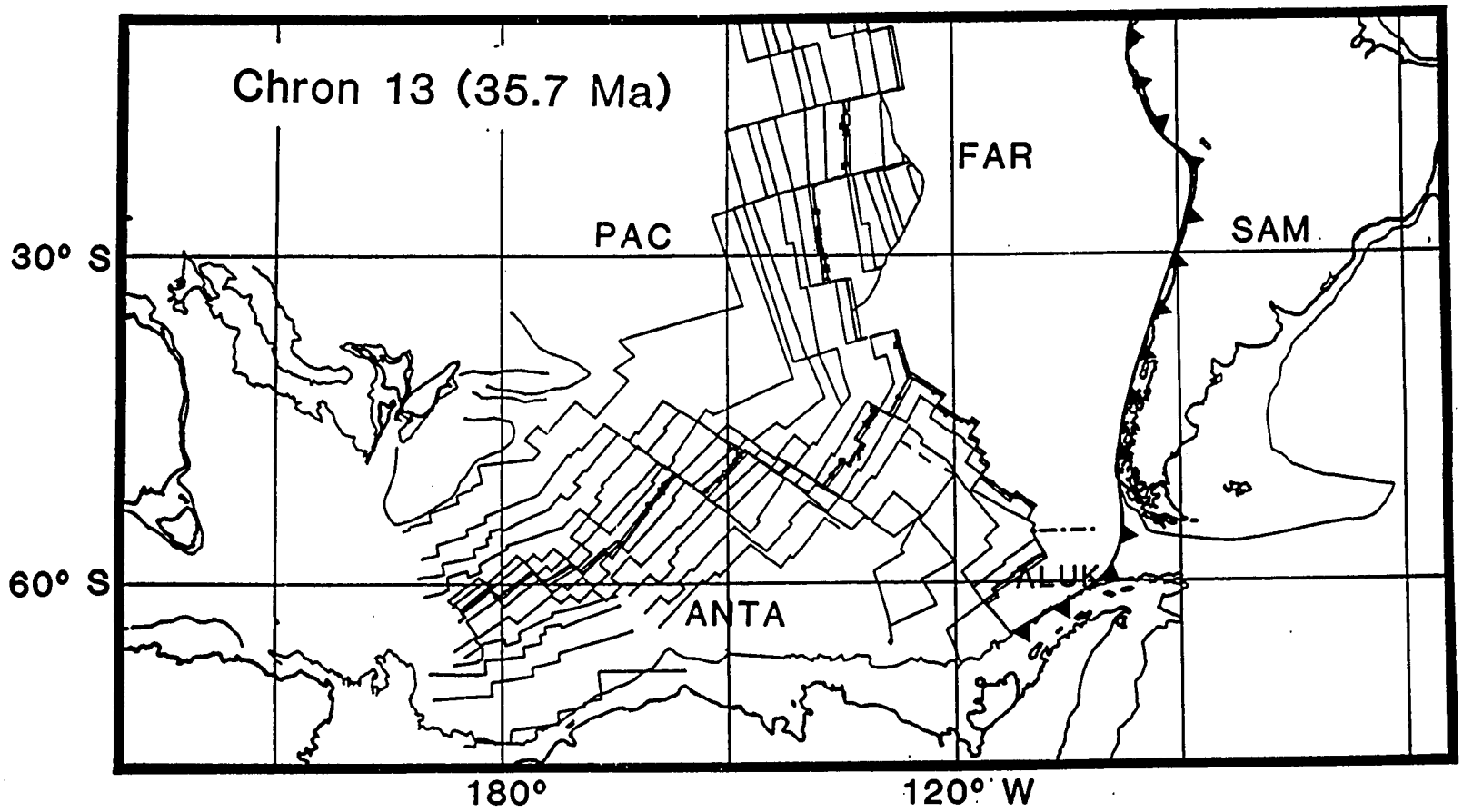
Chron 13 (35.7 Ma)
FAR
PAC
SAM
30° S
60° S
ANTA
ALUK
180°
120° W

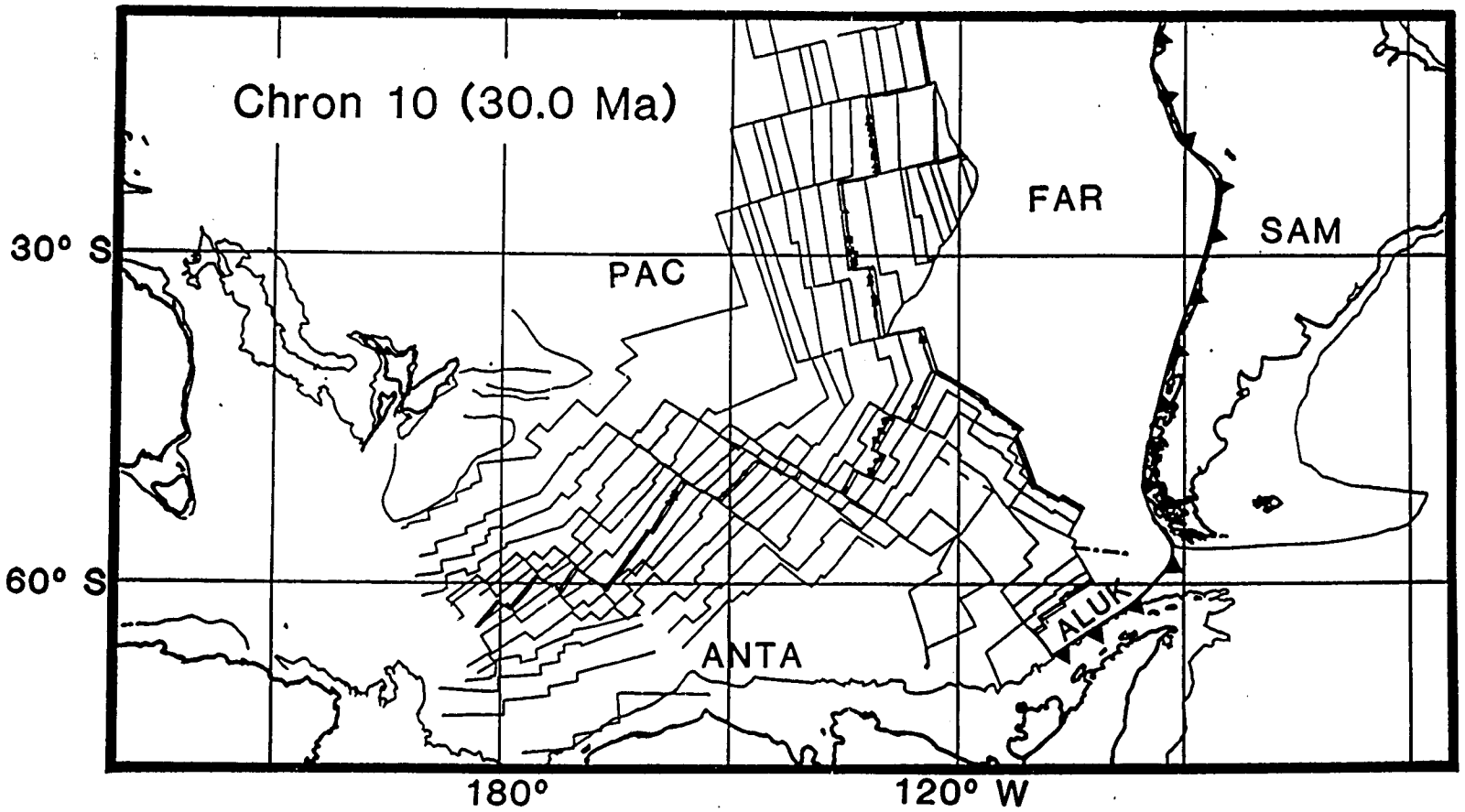
Chron 10 (30.0 Ma)
FAR
SAM
PAC
30° S
60° S
ALUK
ANTA
180°
120° W

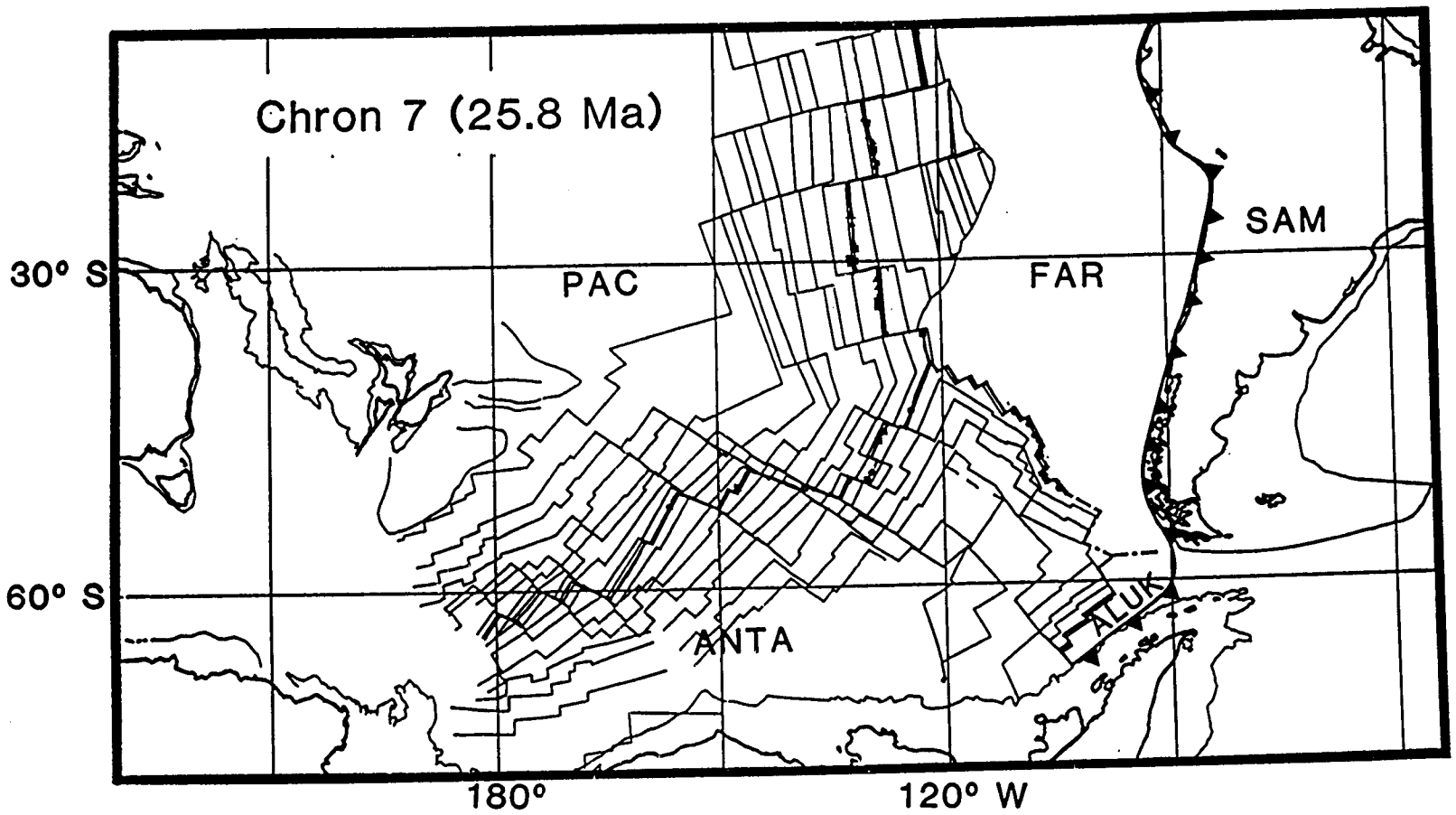
Chron 7 (25.8 Ma)
30° S
60° S
PAC
FAR
SAM
ANTA
ALUK
180°
120° W

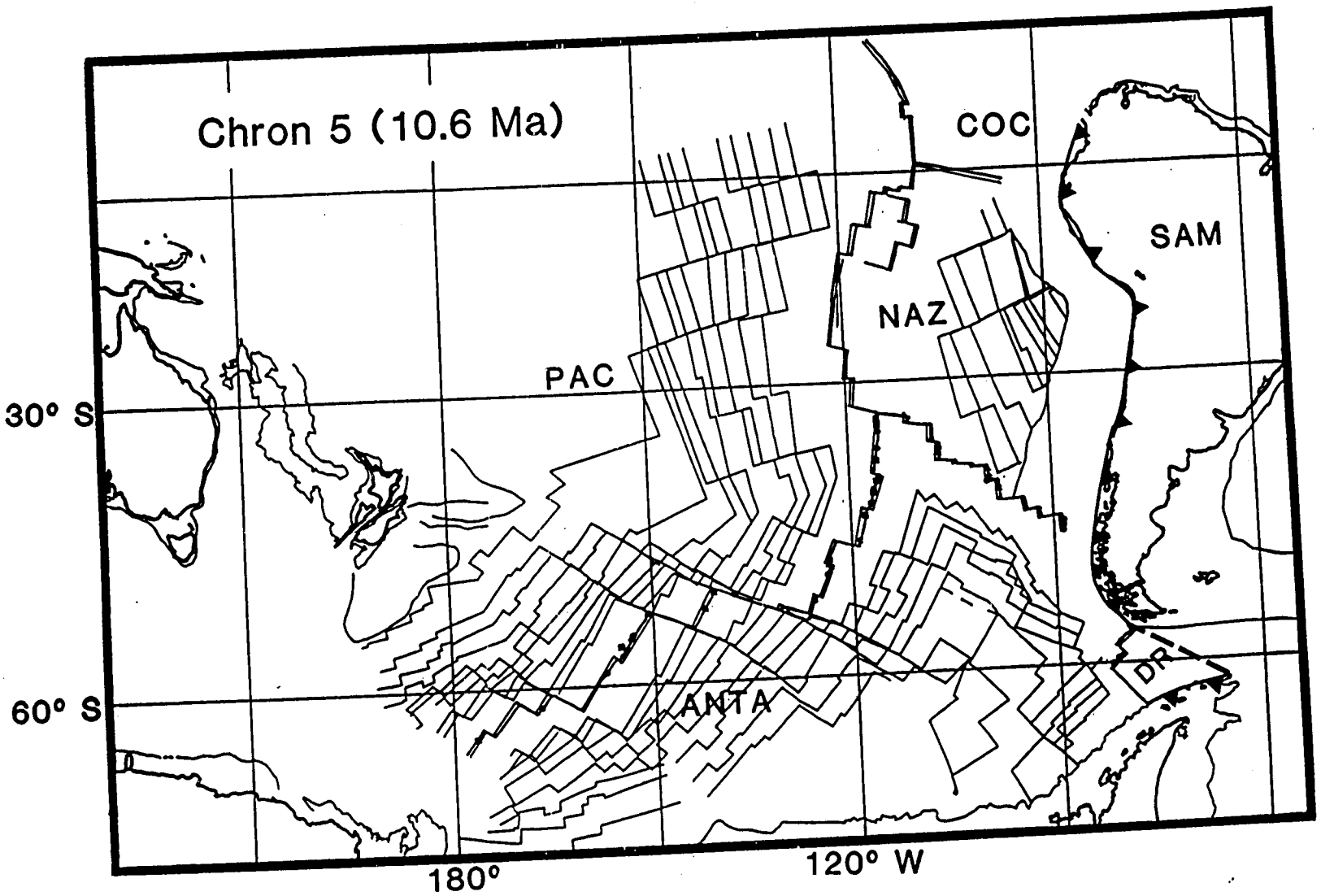
Chron 5 (10.6 Ma)
COC
SAM
NAZ
PAC
30° S
60° S
ANTA
DR
180°
120° W

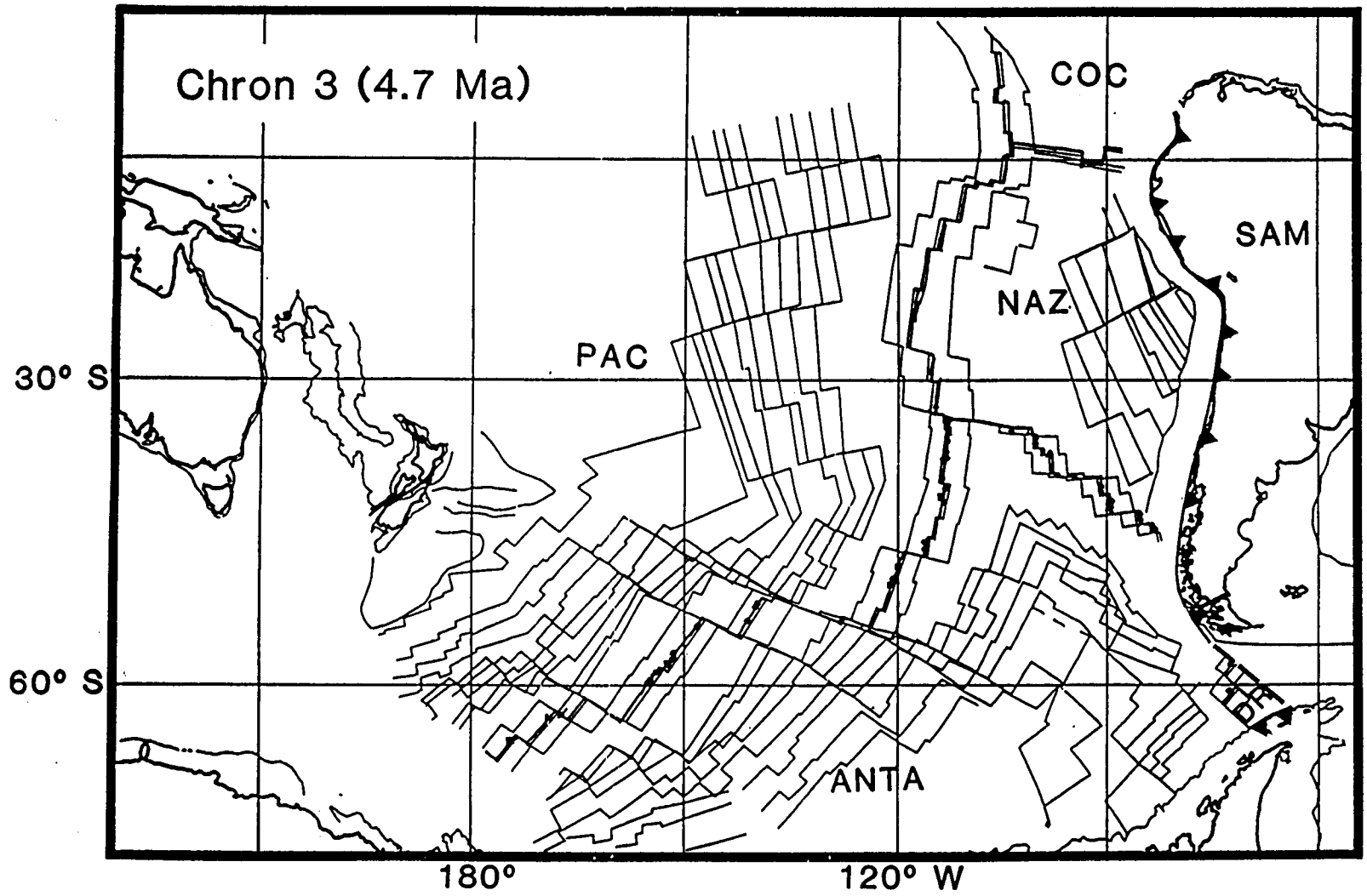
Chron 3 (4.7 Ma)
COC
SAM
NAZ
PAC
30° S
60° S
ANTA
180°
120° W

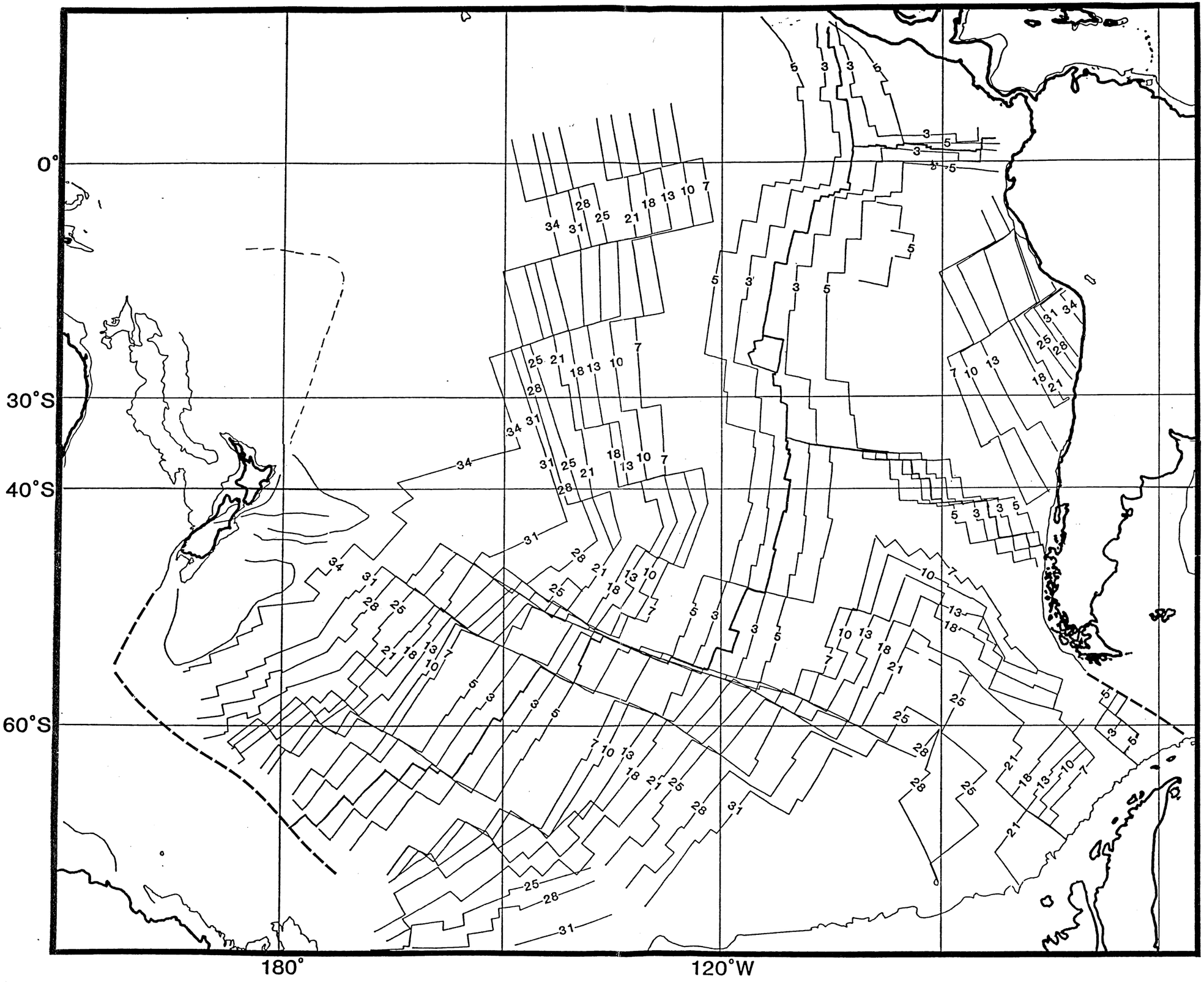
0°
30°S
40°S
60°S
180°
120°W